Research Report

Research Project T9902, Task 28
Floating Bridge Anchor Instrumentation

EXPERIMENTAL RESPONSE AND ANALYSIS OF THE EVERGREEN POINT FLOATING BRIDGE

By

David I. McLean
Professor

Scott T. Peterson
Graduate Student

Washington State Transportation center (TRAC)
Department of Civil and Environmental Engineering
Washington State University
Pullman, Washington, 99164-2910

Washington State Department of Transportation
Technical Monitor
Mark W. Anderson
Design Unit Supervisor

Prepared for

Washington State Transportation Commission
Department of Transportation
and in cooperation with
U.S. Department of Transportation
Federal Highway Administration

March 2003

1. REPORT NO.	2. GOVERNMENT ACCESSION NO.	3. RECIPIENT'S CATALOG NO.
WA-RD 558.1		

4. TITLE AND SUBTITLE	5. REPORT DATE
Experimental Response and Analysis of the Evergreen Point Floating Bridge	March 2003
	6. PERFORMING ORGANIZATION CODE
7. AUTHOR(S)	8. PERFORMING ORGANIZATION REPORT NO.
David I. McLean and Scott T. Peterson	
9. PERFORMING ORGANIZATION NAME AND ADDRESS	10. WORK UNIT NO.
Washington State Transportation Center (TRAC) Civil and Environmental Engineering; Sloan Hall, Room 101 Washington State University Pullman, Washington 99164-2910	11. CONTRACT OR GRANT NO. T9902-28
12. SPONSORING AGENCY NAME AND ADDRESS	13. TYPE OF REPORT AND PERIOD COVERED
Research Office Washington State Department of Transportation Transportation Building, MS 7370 Olympia, Washington 98504-7370	Research Report
	14. SPONSORING AGENCY CODE

15. SUPPLEMENTARY NOTES

This study was conducted in cooperation with the U.S. Department of Transportation, Federal Highway Administration

16. ABSTRACT

On January 20, 1993, the Evergreen Point Floating Bridge incurred structural damage at two mooring cables and at various other locations during a storm event of approximately a 20-year return period magnitude. The two mooring cables damaged were the shorter and stiffer cables located at the ends of the bridge. Following the 1993 storm, larger mooring cables with Sealink elastomeric devices were installed at the areas where cable distress was noted to resist higher cable loads and to provide energy absorption and reduced cable stiffness. In this study, cable forces were measured during the winter season of 2001-2002 to evaluate the effectiveness of the replacement mooring cables. From the experimental measurements, it was found that the special replacement mooring cables have reduced the load attraction at the shorter end cables when compared to cable tension values reported for the pre-retrofit analysis. However, the measurements indicate that the replacement cables continue to attract loads between 64% and 79% higher than those measured at the longer and more flexible cables located near the midspan of the floating bridge during storm events of a 1-year return period magnitude.

17. KEY WORDS	18. DISTRIBUTION STATEMENT
Key words: floating bridge, wave loading, experimental response, Sealink elastomer, mooring cable	No restrictions. This document is available to the public through the National Technical Information Service, Springfield, VA 22616

19. SECURITY CLASSIF. (of this report)	20. SECURITY CLASSIF. (of this page)	21. NO. OF PAGES	22. PRICE
None	None	82	

DISCLAIMER

The contents of this report reflect the views of the authors, who are responsible for the facts and the accuracy of the data presented herein. The contents do not necessarily reflect the official views or policies of the Washington State Department of Transportation, or the Federal Highway Administration. This report does not constitute a standard, specification, or regulation.

TABLE OF CONTENTS

LIST OF FIGURES

LIST OF TABLES

EXECUTIVE SUMMARY

On January 20, 1993, the Evergreen Point Floating Bridge (EPFB) incurred structural damage at two mooring cables and at various other locations during a storm event of approximately a 20-year return period magnitude. The two mooring cables damaged were the shorter and stiffer cables located at the east and west ends of the bridge. Following the 1993 storm, larger diameter mooring cables with Sealink elastomeric devices were installed on the shorter end cables where distress was noted to resist higher cable loads and to provide energy absorption and reduced cable stiffness.

Following installation of the retrofitted mooring cables, the Washington State Department of Transportation (WSDOT) issued a contract to Washington State University (WSU) researchers to evaluate the effectiveness of the Sealink elastomers in reducing the over-stiff effects of the shorter mooring cables on the bridge and to evaluate the distribution of wind and wave loading to the mooring cables along the length of the floating bridge.

Eight of the mooring cables were instrumented to measure cable tension during storm events. Each of the retrofitted cables as well as cables at other locations near the midspan of the bridge were instrumented. The measurements from mooring cables located near the midspan of the bridge allowed an evaluation of the distribution of the environmental loading to the mooring cables along the length of the bridge. Cable forces were measured during 34 storm events that occurred over the winter season of 2001-2002. Of the 34 storm events captured, several of the events were determined to be approximately equal in magnitude to a 1-year return period storm event, while the others were of lesser magnitude.

From the experimental measurements, it was found that the special replacement mooring cables with Sealinks reduced the load attraction at the shorter end cables when compared to cable tension values reported for the pre-retrofit analysis. However, measurements indicate that the replacement cables continue to attract loads between 64% and 79% higher than those measured at the longer and more flexible cables near the midspan during the measured storm events of approximately a 1-year return period magnitude.

Analytical work performed to further investigate the behavior of the replacement mooring cables showed that the retrofitted cables are more flexible than the original cables for loads resulting from a 1-year return period storm event. However, for wind and wave loading expected for larger magnitude storm events, the mooring cable analysis showed that the replacement cables may behave stiffer than the previous cables, resulting in attraction of higher loads at these cables than was experienced prior to retrofit.

The analytical study showed that a true uniform distribution of mooring cable tension forces might not be possible for the mooring system. However, additional reduction in load attraction at the shorter end cables may be obtained by adjusting the pretension values of the end cables differently than for the longer cables located away from the ends of the floating bridge. These additional reductions in load attraction were determined to be approximately of the same magnitude as the reductions obtained through the addition of the Sealink devices to the replacement mooring cables.

INTRODUCTION

INTRODUCTION AND BACKGROUND

Floating bridges have been used to cross bodies of water since the time of the Persian military escapades into southern Europe (Hutchison 1984, Gloyd 1988). However, throughout history, many of the floating bridges built were only temporary structures. Procedures for the design and maintenance of permanent floating bridges have lagged in comparison to the great length of time over which floating bridges have been used. Floating bridge behavior has been a research interest only for the past 60 or so years, mostly in Washington State and in Scandinavia.

The floating bridges typical of those used in Washington State consist of concrete pontoons bolted together end-to-end to form a continuous floating bridge, rectangular in cross section, with the top surface of the closed pontoons serving as the road surface. This type of floating bridge is referred to as a longitudinal pontoon bridge (Lwin 2000). Each of the pontoons is compartmentalized, as is common with many marine vessels and structures, to prevent flooding of an entire pontoon should an outside wall be damaged or punctured. In the transverse or horizontal direction, each of the pontoon sections are held in position through a system of mooring cables connecting the pontoons with anchors located on the lake or sea bottom.

The Washington State Department of Transportation (WSDOT) currently owns and operates four floating bridges: the Hood Canal Bridge on State Route 104, the Lacey V. Murrow Bridge (LVMB) and the Homer M. Hadley Memorial Bridge (HMHMB) providing the I-90 crossing over Lake Washington, and the Evergreen Point Floating

Bridge (EPFB) forming the State Route 520 crossing over Lake Washington between Seattle and Bellevue.

Of the four floating bridges in Washington State, two failures have occurred. The west half of the Hood Canal Bridge failed and sank during a 100-year storm event in 1979, and the original Lacey V. Murrow Bridge sank while under renovation in November of 1990. Since the failure of the Hood Canal Bridge, the WSDOT has directed and funded several research projects in the interest of developing a better understanding of the behavior and response of floating bridges to wind and wave loading and to develop improved procedures for the safe maintenance and operation of the bridges over their expected life.

In addition to the two failures, the EPFB weathered a storm of approximately a 20-year return period event on January 20, 1993 and incurred structural damage at various locations, including two of the southern mooring cables located at the east and west ends of the bridge, cables A_s and AA_s. The shorter mooring cables located at the ends of the floating bridge are stiffer than the longer mooring cables located away from the ends of the bridge. Due to the stiff behavior of the shorter mooring cables, these cables tend to experience higher tension loads during storm events than the longer more flexible cables. Since the mooring system alone provides the lateral restraint of the bridge under wind and wave loading, it is imperative that the integrity of the mooring system be maintained so that the safety of the bridge is not impacted during storm events.

Following the 1993 storm event, two of the mooring cables at each end of the bridge, A_s, B_s, Z_s, and AA_s, were replaced with larger diameter cables connected to Sealink elastomeric energy-absorbing devices. Two Sealink elastomers were added in

series with the larger-diameter replacement cables, located at the anchor end of the cables. A photograph of a Sealink elastomer is shown in Figure 1, and the elastomers were connected to the mooring cables as shown in Figure 2. Design calculations showed that the addition of the two elastomers would reduce the tension loads at the shorter mooring cables to loads similar to those experienced at the longer mooring cables during larger magnitude storm events (The Glosten Associates 1997). The WSDOT issued a contract to Washington State University (WSU) researchers to determine the effectiveness of the Sealink elastomers in relieving the over-stiff behavior of the shorter end cables and to evaluate the distribution of wind and wave loading to the mooring cables along the length of the floating bridge.

Figure 1 – Sealink Elastomer

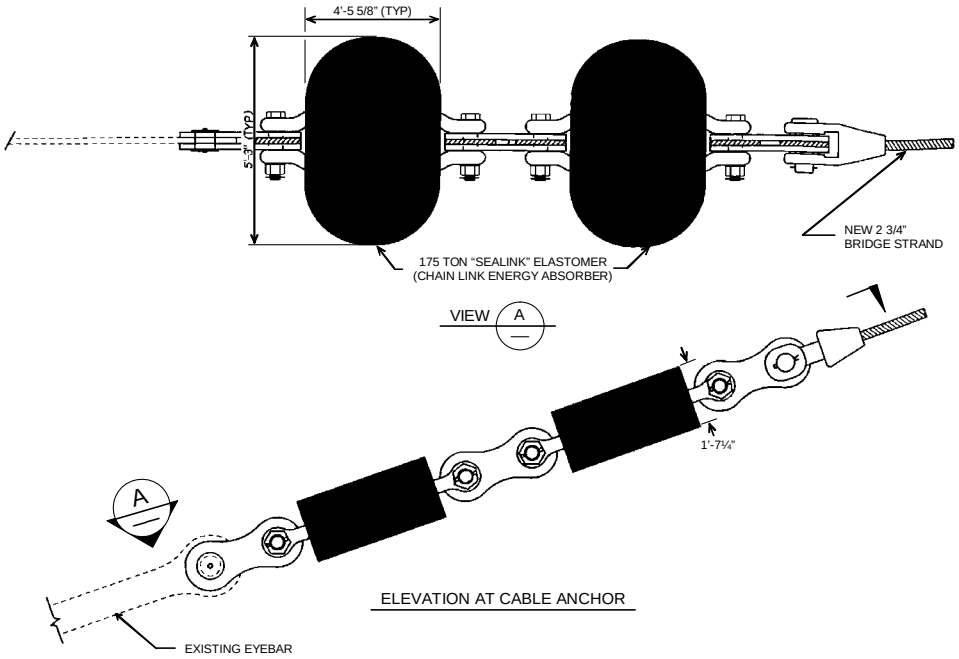

Figure 2 – Elastomers Installed in Series with Mooring Cable

RESEARCH OBJECTIVES

Aligned with WSDOT's long-term research objectives for floating bridges, the current study was conducted to obtain a better understanding of the structural behavior of floating bridges under service load conditions for purposes of evaluation and strengthening of existing floating bridges. To reach this overall goal, three objectives were established: 1) obtain detailed measurements of mooring cable forces, concrete pontoon strains, and overall bridge movements under actual storm conditions, 2) investigate mooring cable forces along the length of the bridge and evaluate the effectiveness of Sealink elastomers, and 3) investigate possible changes to the structural configuration of the bridge that may improve its performance under wind and wave loading.

PREVIOUS RESEARCH AND ANALYSIS APPROACHES

Much of the previous research on floating bridges was conducted in the interest of understanding the response of a floating bridge to wind and wave loading. These studies have resulted in improvements in the ability to model a floating bridge and to determine the extreme structural responses of the bridge under environmental loading. In this section, the previous research is discussed as pertains to the specific methodologies used to model and analyze floating bridges. Other studies have been conducted on various issues that are relevant to the overall understanding of floating bridges, but these studies were not necessarily conducted with floating bridges in mind. These studies will be discussed in other sections of this research report as appropriate.

Continuous floating bridges essentially act as beams on elastic foundations in both the vertical and transverse directions. In the vertical direction, buoyancy provides the linear modulus of the vertical support, while the discrete mooring cables provide the nonlinear horizontal support for the bridge under transverse loading. The design of a floating bridge for traffic is fairly straightforward and typical beam-on-elastic-foundation methods can be used. However, the stochastic structural loading generated by wind and wave action and the corresponding dynamic response of the floating bridge to this loading presents a very complicated system to be understood. The design of a floating bridge for the environmental loading becomes much more difficult than for traffic loading. Despite the complications, understanding must be achieved if an efficient and safe design for a floating bridge is to be obtained.

Significant efforts have been made to understand floating bridge behavior, both experimentally and analytically, by researchers associated with the WSDOT in the years

since the failure of the Hood Canal Floating Bridge as well as by several European researchers and designers. The following discussion presents a brief account of the development of the understanding of floating bridge behavior and corresponding analytical techniques which have been developed, some specifically as a result of research conducted through WSDOT funding and initiative.

The first floating bridges (original LVMB, Hood Canal Floating Bridge, and EPFB) were designed using a simplified technique presented by Stoker (1957) since very little experimental or theoretical work had been done at that time on the dynamic behavior of floating bridges under wind and wave loading (Lwin 1989). The floating bridge was considered as either a rigidly fixed floating beam or as a freely floating beam, and the waves were considered as simple harmonic loading acting on the floating bridge. Stoker's theory was modified to correlate with limited field observations of the existing floating bridges, and an amplification factor was used to account for any resonance effects between the waves and the response of the floating bridge. While the original methods used to determine the structural response of a floating bridge subject to wave loading were relatively straightforward, the methods did not consider the spectral distribution of the wave frequencies and the stochastic nature of the loading, nor the extreme structural responses expected for a given magnitude storm event.

Modern analysis techniques for floating structures subjected to wind and wave loading fall into one of two main categories: time-history analysis or frequency domain spectral analysis. For brevity, only a brief description of each will be discussed below as well as the main advantages and disadvantages of the two analysis methods. For additional details concerning the two analysis techniques, see Peterson (2002).

TIME-HISTORY ANALYSIS

For a time-history analysis of a floating bridge, six degrees of freedom are typically considered. The translational degrees of freedom in the longitudinal, lateral, and vertical directions are referred to as surge, sway, and heave, respectively. The rotational degrees of freedom about the longitudinal, lateral, and vertical axes are referred to as roll, pitch, and yaw, respectively. The degrees of freedom considered for the structural model of a floating bridge are shown in Figure 3.

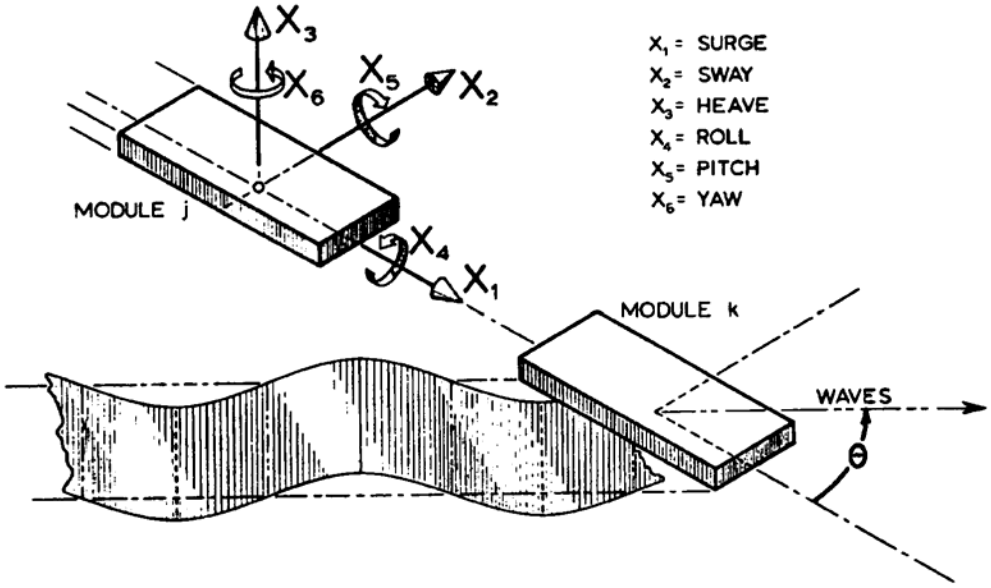

Figure 3 – Coordinate System and Degrees of Freedom for Structural Model
Figure Obtained from Hutchison (1984)

The structural model is generated using beam elements to represent the concrete pontoons and cable elements to represent the mooring system. Equations of motion for each of the degree of freedom considered are formed considering all structural and hydrostatic or hydrodynamic contributions. These equations are then integrated to

determine the forces and displacements such that dynamic equilibrium is satisfied at each time step considered. From these forces and displacements, the maximum structural response quantities are determined and used for design calculations.

The main advantages of the time-history method of analysis are the ability to consider the nonlinear stiffness effects of the mooring cables and the ease of interpretation of the maximum structural response quantities. The nonlinear stiffness effects of the mooring cables can only be considered using a time-history analysis. In addition, time-history analysis directly yields the extreme response quantities such as maximum cable tension or maximum bending moment.

The time-history method of analysis also has some limitations in that the hydrodynamic mass and damping coefficient terms must be considered constant while the hydrodynamic coefficients are in fact frequency dependent (Isaacson and Sarpkaya 1981, The Glosten Associates 1991a). However, since the bandwidth of the spectral density of the response quantities is typically narrow, the assumption of constant hydrodynamic coefficient terms can be made with acceptable levels of error (Langen and Sigbjörnsson 1980, Hartz 1981). In addition, time-history analyses must be made for long periods of simulation time in order to capture the extreme structural response likely to occur during a particular storm event. Studies have also shown that different simulations of similar magnitude wave loading applied used for a time-history analysis may produce quite different results in terms of the extreme response of the floating bridge under a given magnitude storm event (Liu and Bergdahl 1998). Thus, either a very long simulation or several simulations of moderate length may be required to fully capture the extreme values of the structural response to the stochastic loading from wind and waves.

FREQUENCY DOMAIN ANALYSIS

As an alternative to a time-history analysis of a floating bridge, the analysis may be considered in the frequency domain where a spectral analysis follows (Langen and Sigbjörnsson 1980, Hutchison 1984). The equations of motion are written in much the same way as for a time-history analysis, but the equations are transformed from a system of differential equations to a system of complex algebraic equations. The analysis is also separated into two independent analyses which, when combined, give the total structural response quantities of interest. These two analysis segments are the analysis for steady or slowly-varying wind and wave drift loading, and the analysis for the dynamic wave loading acting on the floating bridge (referred to as a perturbation analysis by The Glosten Associates (1991a)). The response quantities determined from each segment are combined statistically to obtain the total structural response.

There are three main benefits to conducting the analysis in the frequency domain. First, the randomness or stochastic nature of the structural loading produced by many waves of varying height and frequency may be preserved in the wave spectrum without the need to generate a long time-history of loading to capture the variation in the loading process. Second, the hydrodynamic properties (added mass and added damping) are frequency dependent, and this method of analysis allows a more exact treatment of the fluid effects on the structure. Finally, the differential equations of motion can be solved as complex algebraic equations in the frequency domain, greatly simplifying the solution process.

As with any mathematical model of a complicated structure, the frequency domain analysis also has some drawbacks. First, the nonlinearities corresponding to the

mooring cables must be linearized to solve the equations of motion for the model in the frequency domain. The perturbation analysis also assumes that the response of the structure corresponding to the dynamic loading is small in comparison to the response to steady or slowly-varying loading. If this is true for the particular structure and loading considered, then the linearization of the mooring cable response may be a good approximation and the perturbation analysis will likely give good results. However, if the response of the structure to dynamic loading is large in comparison to the response to steady loading, the perturbation model may not yield valid results since the linearization of the nonlinear structural components may no longer be a good approximation of the true behavior.

The second main disadvantage to the frequency domain analysis is the necessity for the statistical combination of the results from the slowly-varying load analysis with the response from the perturbation analysis. Many statistical methods have been presented in the literature for combining the responses of a ship or structure to steady and dynamic loading (Ochi 1973, Liu & Bergdahl 1998, Liu & Bergdahl 1999), yet there remains some uncertainty concerning the accuracy in the combination of responses for a floating bridge (The Glosten Associates 1991a).

RESEARCH APPROACH AND PROCEDURES

To achieve the research objectives of this study, cable tension measurement devices were developed and installed on eight of the EPFB mooring cables. In addition, strain gage instruments were installed inside a single pontoon to measure concrete strains during storm events. Instrument signals were collected and recorded through a data acquisition system designed specifically for this project. The selection and installation of instruments and the design of the data acquisition system are discussed in the following sections.

In addition to the experimental work conducted on the bridge, the retrofitted mooring cables were also considered analytically to provide additional understanding of the replacement mooring cables. Finally, a parametric study was also conducted to investigate the effects on the structural response due to adjustments to the configuration of the mooring system. This parametric study was performed in the interest of possible further improvements to the performance of the floating bridge.

EPFB INSTRUMENTATION

Data Acquisition

Collection of the cable tension and concrete strain measurements was made through two custom data acquisition systems designed and installed on the bridge by Measurement Technology Northwest. The two data acquisition systems were installed inside pontoon R and pontoon I and transmitted data via radio frequency to a project-designated computer located at Measurement Technology Northwest's office in Seattle. The acquisition system was programmed to continuously monitor each of the

tensiometers and strain gages as well as the wind speed measurements recorded by the anemometer located on the roof of the bridge control tower. When the wind speed exceeded 40 km/hr for 30 seconds, the data acquisition system began recording the measurements of structural response. Data acquisition was programmed to stop recording and begin monitoring again when the storm subsided and wind speeds dropped below 32 km/hr for longer than 5 minutes. The project-designated computer collected measurements transmitted by the data acquisition systems and wrote a data file to the hard drive. When the storm subsided, the computer compressed and automatically emailed the data file to WSU researchers.

Experimental measurements were made at 1 second sampling intervals so that the dynamic response of the floating bridge could be obtained from the measurements. With 1 second sampling intervals, frequencies of vibration of up to 0.5 Hz can be obtained from the measurements. Based on previous analytical frequency studies of the floating bridges on Lake Washington, this sampling interval was determined to be sufficient for this project (The Glosten Associates 1991a).

Mooring Cable Tension

Several different instruments were reviewed in the selection process for the instruments to be used to measure the mooring cable tension. These included tension links, custom-designed triple-yoke instruments, and tensiometers. The tension links were not selected because it was necessary to sever the mooring cables and install the links in series with the cable, which was determined to be a costly operation. Custom-designed triple-yoke instruments were used previously on the Hood Canal Bridge (The Glosten Associates 1984). However, the Hood Canal mooring cables are configured in a side-by-

side configuration, differently than the EPFB mooring cables. The configuration of the EPFB mooring cables did not allow the triple-yoke instruments to be used. Tensiometer instruments, designed and manufactured by Houston Scientific International, Inc. were selected for use on the EPFB since the instruments were developed specifically for the measurement of mooring cable tension and did not require that the cable be severed to install the instruments. A photograph of one of the tensiometer instruments is show in Figure 4.

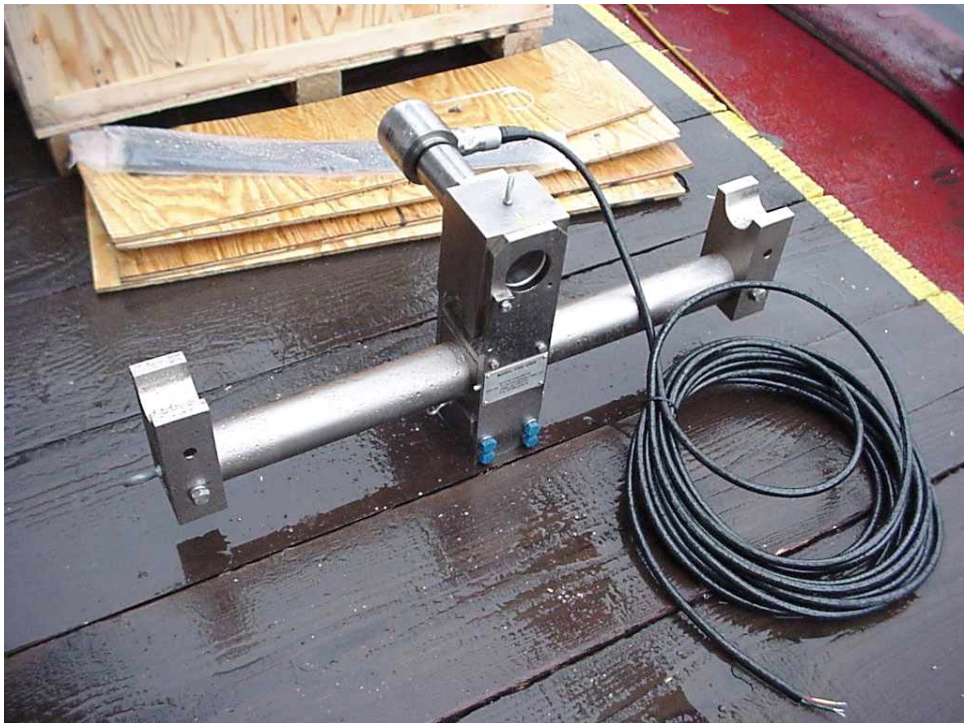

Figure 4 – Tensiometer Instrument

To determine the effectiveness of the Sealink elastomers in reducing the stiffness of the replacement mooring cables, instrumentation was installed on the retrofitted mooring cables A_s, B_s, Z_s, and AA_s. In addition to the retrofitted cables, instrumentation was also installed on cables C_s, I_s, R_s, and Y_s. The additional cables were selected to determine the effects on the adjacent mooring cables (cables C_s and Y_s) due to the

addition of the Sealink elastomers as well as to assess the distribution of wind and wave forces to the mooring cables located along the length of the bridge.

The eight tensiometer instruments were installed on the selected mooring cables on December 21, 1999 at a water depth of approximately 3 to 5 meters. On the day of installation, it was noted that discrepancies existed between the cable tension measurements obtained from the tensiometers and the cable pretension values set by the WSDOT pretensioning system. For a few of the cables, the discrepancies were on the order of 35% of the measurements obtained.

Three extensive sets of tests were conducted to determine the source of the discrepancy. Tests were performed by loading and unloading the instrumented cables using the WSDOT pretensioning system while simultaneously recording cable tension measurements from the tensiometers, the WSDOT hydraulic jacking system and an in-line load cell. Comparisons showed that the measurements obtained from the WSDOT hydraulic jacking system yielded tension measurements and cable behavior that agreed more closely with that expected from theory. After evaluating results from these tests, it was concluded that the tensiometer readings were in error despite the laboratory calibrations performed with the tensionmeters on samples of the mooring cables.

Following the tests, the calibration curves for each of the eight tensiometers were adjusted numerically such that the measurements obtained from the tensiometer instruments agreed with the measurements obtained from the WSDOT pretensioning system during the tests. These numerical corrections were then applied to the measurements obtained from the tensiometers during the captured storm events of the 2001-2002 winter season. Table 1 shows the percent difference values between the cable

tension measurements obtained from the tensiometers and the WSDOT hydraulic jacking system before and after correction of the tensiometer measurements. Since the WSDOT pretensioning system was determined to yield correct measurements of cable tension, the percent difference values are presented as percent error in the tensiometer measurements with respect to the WSDOT measurements. The percent error values for the corrected readings are very reasonable for field measurements.

Table 1 - Error in Corrected Tensiometer Measurements Compared to WSDOT

Cable	Uncorrected Tensiometer		Corrected Tensiometer	
	Max Error (%)	Avg. Error (%)	Max Error (%)	Avg. Error (%)
A_s	24.33	12.77	13.26	5.26
B_s	11.55	4.12	5.45	2.26
C_s	14.95	10.46	2.72	0.92
I_s	36.13	33.19	6.79	1.38
R_s	34.76	28.86	5.29	1.58
Y_s	11.99	5.05	4.54	2.02
Z_s	11.46	5.85	2.57	1.01
AA_s	10.63	5.46	8.30	2.25

Concrete Pontoon Strains

In addition to the cable tension measurement instrumentation, 26 strain gages were installed inside pontoon R to measure the concrete strain response during the storm events captured. Fourteen of the 26 strain gages were configured to measure flexural strains, while the remaining 12 gages were configured to measure shear strains. The specific gages selected were full-bridge strain gage instruments with a gage length of 51

mm. These instruments were determined to be the best suited for use inside the concrete pontoons through a pilot study conducted during October of 2000.

The 26 gages were located around the interior perimeter of pontoon R, located halfway between the anchor gallery and the eastern end wall. This location was selected to avoid possible anomalous strain behavior near the anchor gallery and end walls. The locations of the flexural and shear strain gages are shown in Figures 5 and 6, respectively.

Despite efforts to obtain meaningful measurements of concrete strains and interpret these measurements to better understand the response of the pontoons, a number of complicating issues prevented the full interpretation of the measurements. These included shifting baseline strain gage signals with changes in temperature and lake water level that prevented the determination of absolute measurements of strain. Despite the complications, some conclusions were made based on the strain measurements from a relative perspective and are discussed later in the section entitled Findings and Discussion.

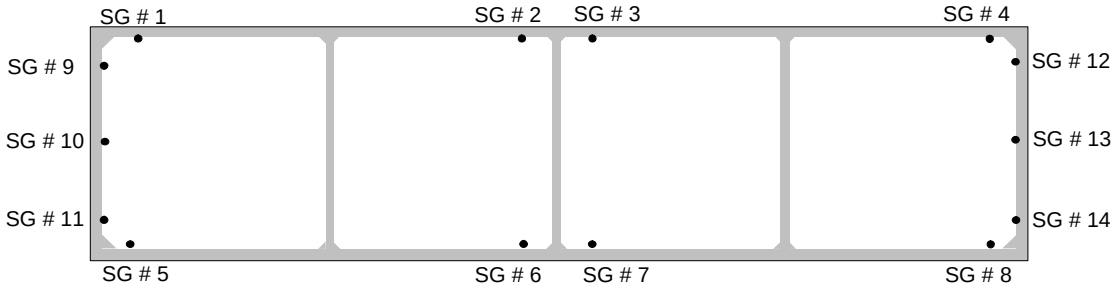

Figure 5 – Locations of Flexural Strain Gages

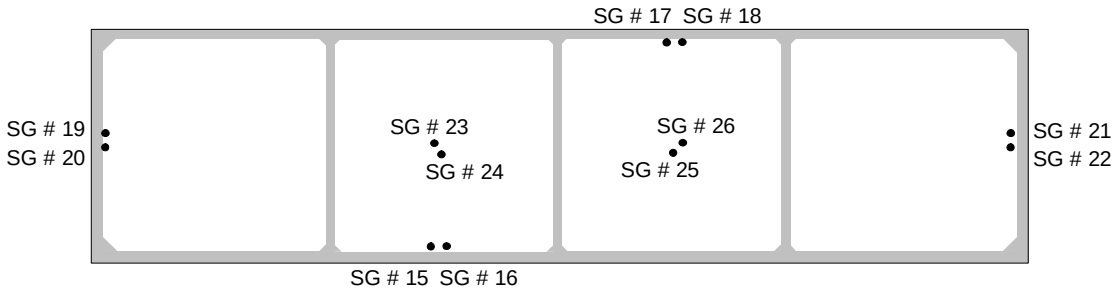

Figure 6 – Locations of Shear Strain Gages

Differential GPS Measurements of Bridge Motion

In addition to the cable tension and pontoon strain measurements, arrangements were made with the WSDOT Surveying Department to obtain measurements of the EPFB motion during up to three storm events through differential global positioning system (DGPS) measurements of the position of the bridge at several locations. Despite the planning and arrangements made with the WSDOT Surveying personnel to obtain the DGPS measurements during several storm events, they were never obtained. However, the plans made to obtain the measurements and the rationale behind the locations of receivers are discussed to provide information on what plans were made in the past and what may be available in the future to obtain DGPS measurements of the bridge response during storm events.

Three different configurations were developed in which 7 GPS receivers were to be attached to the bridge at various locations. During a particular significant storm event, the WSDOT Surveying Department was to attach the GPS receivers to prefabricated mounts and obtain 3-dimensional measurements of the position of the bridge at 1 second sampling intervals with an accuracy of approximately 1 to 2 cm. The receivers were located such that the overall displaced shape of the bridge could be measured as well as

the dynamic motion of a more focused section of the floating bridge. More information on the details of each of the DGPS configurations is available in Peterson (2002).

STATISTICAL ANALYSIS OF CABLE TENSION MEASUREMENTS

During the winter of 2001-2002, the structural response of the mooring cables A_s, B_s, C_s, I_s, R_s, Y_s, Z_s, and AA_s on the bridge were measured during a total of 34 storm events. For the 34 storm events, the peak instantaneous wind speeds ranged between 40 and 103 km/h. Given the previous statistical determinations of the return period storm events of interest in the design and maintenance of the floating bridges on Lake Washington (The Glosten Associates 1991a, 1993a), the measured storm events fell in a range generally below the 1-year storm event, with the exception of three storms which were approximately equal to the 1-year event. Table 2 summarizes the wind speed measurements and duration of each of the 34 storm events recorded as well as calculated values for wave height, wave period and wave frequency. The calculated wave parameters were obtained using the computer program NARFET developed by the U.S. Army Corps of Engineers (1989).

Using the recorded cable tension measurements, a statistical evaluation of the structural response of the bridge mooring cables was performed. The simplest statistical evaluation to be made, but perhaps of the highest interest, is the evaluation of maximum cable tension measured during the storms. The maximum values of cable tension measured during the captured storm events are listed in Table 3.

Table 2 – Storm Records Obtained During Winter 2001-2002

Storm Record		Peak (Instant.) Wind Vel. (km/h)	Fastest Mile Wind Vel. @ 44.09 ft (km/h)	Avg Wind Heading (deg az)	Wave Height H_{mo} (m)	Wave Period T_m (s)	Wave Freq. f (Hz)	Storm Duration (hrs)
1	10/23/01 00:15	82	65	28.6	0.59	2.76	0.36	5.86
2	10/30/01 17:01	76	64	22.5	0.60	2.77	0.36	18.20
3	11/15/01 14:36	48	40	18.2	0.36	2.22	0.45	2.25
4	11/19/01 20:56	90	72	20.5	0.69	2.95	0.34	8.51
5	11/20/01 21:32	55	46	17.3	0.42	2.37	0.42	1.13
6	11/21/01 00:32	56	48	21.2	0.44	2.41	0.41	8.27
7	11/23/01 08:06	43	36	20.6	0.32	2.09	0.48	3.17
8	11/26/01 18:36	40	37	19.8	0.32	2.11	0.47	0.96
9	11/29/01 03:19	60	52	21.4	0.48	2.5	0.40	6.76
10	11/29/01 17:28	47	38	20.5	0.34	2.15	0.47	4.92
11	11/30/01 03:47	60	45	20.2	0.41	2.33	0.43	1.56
12	11/30/01 06:30	56	47	20.3	0.43	2.39	0.42	6.28
13	11/30/01 14:02	50	45	18.9	0.40	2.32	0.43	1.71
14	12/01/01 04:58	74	63	19.2	0.59	2.75	0.36	7.91
15	12/01/01 13:04	103	85	20.4	0.84	3.21	0.31	15.23
16	12/03/01 16:05	71	58	20.3	0.53	2.64	0.38	9.77
17	12/04/01 10:56	56	47	21.8	0.42	2.37	0.42	7.65
18	12/04/01 19:30	47	39	18.9	0.35	2.19	0.46	1.51
19	12/05/01 16:04	47	39	19.4	0.35	2.18	0.46	3.22
20	12/06/01 05:00	71	59	20.7	0.54	2.65	0.38	5.53
21	12/08/01 12:31	72	57	21.5	0.52	2.6	0.38	5.64
22	12/12/01 22:50	72	60	20.5	0.55	2.67	0.37	4.48
23	12/13/01 04:43	69	55	22.5	0.50	2.57	0.39	1.72
24	12/13/01 09:45	64	57	20.5	0.52	2.61	0.38	1.92
25	12/13/01 16:27	92	80	22.4	0.78	3.11	0.32	8.53
26	12/16/01 18:27	80	68	21.2	0.64	2.86	0.35	4.27
27	12/17/01 02:27	80	70	22.5	0.66	2.89	0.35	1.72
28	12/18/01 15:08	82	67	21.5	0.62	2.83	0.35	7.49
29	3/05/02 02:07	71	60	31.2	0.53	2.63	0.38	1.97
30	3/08/02 14:14	55	47	23.0	0.42	2.38	0.42	5.74
31	3/09/02 22:06	53	44	23.7	0.39	2.3	0.43	1.06
32	3/10/02 14:12	72	62	33.3	0.55	2.67	0.37	6.89
33	3/26/02 09:58	68	57	31.9	0.51	2.57	0.39	9.13
34	3/27/02 13:02	72	60	28.7	0.54	2.64	0.38	16.70

Table 3 – Maximum Cable Tension Measurements

Storm Record	Maximum Cable Tension Measurements							
	Cable A_s (kN)	Cable B_s (kN)	Cable C_s (kN)	Cable I_s (kN)	Cable R_s (kN)	Cable Y_s (kN)	Cable Z_s (kN)	Cable AA_s (kN)
1	775	698	737	644	684	750	786	825
2	812	682	715	647	681	716	788	830
3	718	596	569	535	540	521	548	469
4	1146	896	728	668	655	658	705	773
5	522	542	516	500	529	489	516	454
6	586	555	543	527	548	521	548	499
7	812	695	569	516	564	525	574	549
8	447	480	460	467	502	444	481	431
9	653	626	563	503	527	504	535	498
10	461	486	468	472	503	449	489	448
11	512	516	488	475	505	453	490	435
12	639	541	506	504	520	457	541	502
13	542	515	469	472	499	448	490	454
14	917	692	596	554	575	548	618	628
15	1211	885	790	633	682	718	846	927
16	765	646	544	519	537	479	536	549
17	694	574	506	498	511	452	519	486
18	474	482	458	463	493	433	476	428
19	454	469	453	457	494	432	466	418
20	718	561	546	533	552	516	622	686
21	646	568	530	510	556	527	589	686
22	754	585	568	551	616	557	647	706
23	536	533	521	495	546	522	609	619
24	670	556	516	509	538	495	554	542
25	935	723	691	661	713	803	969	1125
26	959	832	666	592	647	628	691	733
27	692	610	590	560	627	638	717	801
28	863	685	616	556	596	540	622	630
29	703	669	676	617	654	685	730	709
30	647	668	660	604	648	664	695	618
31	632	673	680	605	644	689	689	602
32	737	695	723	647	682	718	750	712
33	880	866	881	760	786	899	900	902
34	912	868	909	774	807	937	930	935

Other statistical evaluations of the cable tension measurements of interest are the evaluation of mean and standard deviation of cable tension measured during the storms along with a determination of the statistical distribution that best describes the measurements. Tables of mean and standard deviation values are available in Peterson (2002). Statistical analysis of the time-series tension measurements showed that a normal distribution described the measured data best among normal, lognormal, extreme type I, and extreme type II distributions. It follows that the response of the mooring cable behavior during storm events can be described by the mean, T_M, and standard deviation, T_{STDEV}, of the time-series cable tension measurements.

It is preferable to maintain the use of T_M and T_{STDEV} since both hold physical meaning in the understanding of the response of the mooring cables. More specifically, the difference between the mean cable tension and the cable pretension, denoted T_{M-To} (where T_o represents the cable pretension), was used in to interpret the physical response process measured during the 2001-2002 storm events. Cable pretension values were obtained automatically by the data acquisition system during times when the monitored wind speeds were calm, providing up-to-date cable pretension values throughout the 2001-2002 winter season. The term T_{M-To} corresponds to the response of the bridge to slowly varying wind and wave loading, while T_{STDEV} corresponds to the variation in cable tension about the mean due to dynamic wave loading. Figure 7 shows a segment of a time-history record of cable tension measurements obtained during storm record 33. The cable pretension value shown represents the cable tension measurements obtained during at-rest conditions.

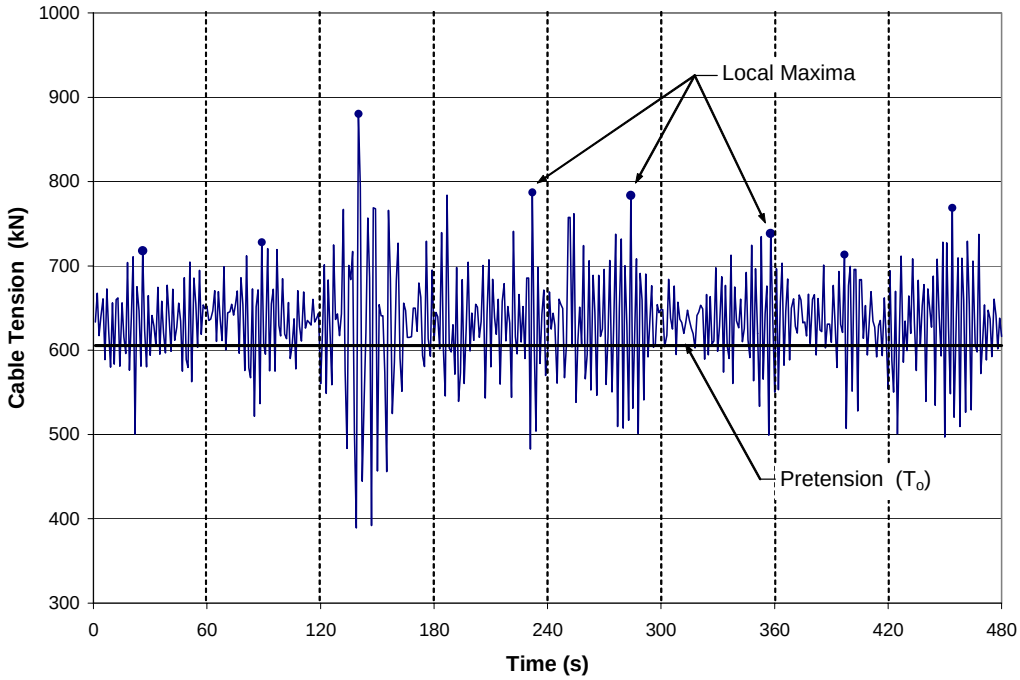

Figure 7 - Time-Series Cable Tension Measurements

The general statistical combination of the mean and standard deviation shown in Equation 1 is typically used to determine the extreme values for a response process (time series) that follows a normal distribution. The statistical combination of the response parameters is shown inside the brackets.

$$T^{p}_{\max} = T_o + \left[T_{M-To} + ZT_{STDEV}\right] \qquad \text{(Equation 1)}$$

T^{p}_{max} is the predicted maximum cable tension value corresponding to the confidence level given by the selected value for the standard normal variate, Z. Equation 1 may seem redundant due to the subtraction and addition of the cable pretension term, T_o. This was done since the terms $T_{M\text{-}To}$ and T_{STDEV} both depend on the wind and wave loading acting on the bridge while the cable pretension is independent of this loading. The terms $T_{M\text{-}To}$ and T_{STDEV} are later expressed as a function of the environmental loading and $T_{M\text{-}To}$ was considered independently of T_o for this reason.

A review of relevant literature shows that while the response process is expected to follow a Gaussian or normal distribution, the extreme values of cable tension *cannot* be obtained through the standard statistical combination of $T_{M\text{-}To}$ and T_{STDEV} for a given level of confidence as shown in Equation 1 (Ochi 1973, Liu and Bergdahl 1999). In using $T_{M\text{-}To}$ and T_{STDEV} to obtain the maximum cable tension value through Equation 1, the fundamental underlying statistical assumption of independent random variables is violated. This is true since the time-series describes a physical process in which the cable tension value at time $t + \Delta t$ is strongly dependent on the tension value at time t (for small values of Δt), and the values are therefore not independent random variables. However, as noted previously, it is preferable to maintain the physical understanding of the structural response described by $T_{M\text{-}To}$ and T_{STDEV}. Therefore, additional statistical work was done to enable the use of $T_{M\text{-}To}$ and T_{STDEV} while obtaining a correct prediction of the extreme or maximum cable tension.

To correctly consider the mooring cable tension measurements from a statistical standpoint, independent local maxima were selected from the time-series measurements. Local maxima separated sufficiently in time have little dependence on each other, and the collection of local maxima can be considered statistically without violating the assumption of independent random variables. For the response of the bridge, time intervals 60 seconds in length were chosen for the selection of local maxima since an EPFB frequency analysis showed that the bridge undergoes approximately 20 full oscillations in 60 seconds. The 60 second intervals are shown in Figure 7 as well as the local maxima selected from each. The collection of local maxima was analyzed statistically, and the extreme type I (Gumbel) distribution was found to describe the

selected local maxima best of the statistical distributions considered. A Gumbel factor, G_F, was calculated corresponding to a given level of confidence to be used in place of the standard normal variate, Z, in combining $T_{M\text{-}To}$ and T_{STDEV} from the measurements. Equation 2 shows the substitution of G_F for the term Z given in Equation 1.

$$T_{\max}^{p} = T_o + \left[T_{M-To} + G_F T_{STDEV}\right] \qquad \text{(Equation 2)}$$

90% Confidence: $G_F = 3.93$

99% Confidence: $G_F = 6.74$

For the 34 storm events recorded during the winter 2001-2002 season, the 99th percentile cable tension values were calculated for each of the 8 instrumented cables and found to predict values that are from 3.5% to 15.4% higher (more conservative) than the actual measured maximum cable tension values.

ENVIRONMENTAL LOADING FACTOR

The overall intent of the data analysis was to obtain a relationship between some measure of the storm conditions and the tension measured at the instrumented cables. To achieve this, wind speed and wind direction measurements were recorded from the weather station located at the bridge control tower synchronized with the cable tension measurements. Several empirical relationships were investigated between various forms of the cable tension and wind speed measurements. The best relationship for the prediction of observed cable tension was obtained through curve fitting $T_{M\text{-}To}$ and T_{STDEV} values versus a term referred to as the environmental loading factor. The environmental loading factor was based on both the magnitude of predicted wave height and the dynamic interaction between the waves and the bridge. It should be noted that the only variables in the determination of a single-valued environmental loading factor

representing an observed storm event are the wind speed and wind direction measured during the 34 observed storm events.

To calculate the environmental loading factor for a particular observed storm event, the energy-based wave height, H_{mo}, is first calculated using the program NARFET (U.S. Army Engineer Waterways Experiment Station 1989). The NARFET program follows the methodology described in the Shore Protection Manual and is based on research conducted in the Puget Sound and elsewhere (Coastal Engineering Research Center 1984, Smith 1991). Using the wind speed, wind duration, and data describing the open water environment surrounding the EPFB, NARFET calculates the energy-based wave height H_{mo}, the wave period T_m, and the central heading angle of the waves. The calculated wave parameters associated with the 34 captured storm events are listed in Table 2.

Wave direction should also be considered in the description of the environmental loading experienced at the bridge, but there is no consensus among researchers familiar with Washington's floating bridges in terms of the appropriate mathematical consideration to be made. For this reason, the central wave heading angle was neglected for the observed storm events. Furthermore, the predicted central heading angles for the observed storms were all nearly normal to the bridge.

In addition to the energy-based wave height, the frequency content of the wave loading was considered. A displacement-based dynamic response factor (Chopra 1995) was used to consider the effects of the dynamic wave loading and evaluate any amplification in structural response that may occur should the wave period approach the

natural period of the bridge. Calculation of the dynamic response factor, R, was made according to Equation 3.

$$R = \frac{1}{\sqrt{\left[1-\left(\frac{f}{f_n}\right)^2\right]^2 + \left[2\xi\left(\frac{f}{f_n}\right)\right]^2}} \qquad \text{(Equation 3)}$$

In this equation, f is the forcing frequency of the wave loading (equal to $1/T_m$), f_n is the natural frequency of the bridge nearest to the forcing frequency, and ξ is the equivalent damping ratio of the bridge.

Finally, using the predicted wave height, H_{mo}, and the calculated dynamic response factor, R, the environmental loading factor (ELF) is calculated according to Equation 4. Environmental loading factors corresponding to general storm events for a given return period are listed in Table 4. Table 5 shows environmental loading factors for the 34 recorded storm events of the 2001-2002 winter season.

$$ELF = RH_{mo} \qquad \text{(Equation 4)}$$

Table 4 – ELF Values for Return Period Storm Events

Return Period	ELF (m)
1 year	1.73
20 year	2.46
100 year	2.82

Table 5 – Environmental Loading Factor for 2001-2002 Storm Records

Storm Record		Frequency Ratio $\beta = f/f_n$	Response Factor R	Wave Height H_{mo} (m)	Environmental Loading RH_{mo} (m)
1	10/23/01 00:15	1.04	1.91	0.59	1.13
2	10/30/01 17:01	1.03	1.92	0.60	1.16
3	11/15/01 14:36	1.29	1.09	0.36	0.39
4	11/19/01 20:56	0.97	2.05	0.69	1.41
5	11/20/01 21:32	1.21	1.33	0.42	0.56
6	11/21/01 00:32	1.19	1.39	0.44	0.61
7	11/23/01 08:06	1.37	0.90	0.32	0.29
8	11/26/01 18:36	1.35	0.93	0.32	0.30
9	11/29/01 03:19	1.14	1.54	0.48	0.73
10	11/29/01 17:28	1.33	0.99	0.34	0.33
11	11/30/01 03:47	1.23	1.26	0.41	0.51
12	11/30/01 06:30	1.20	1.36	0.43	0.58
13	11/30/01 14:02	1.23	1.24	0.40	0.50
14	12/01/01 04:58	1.04	1.90	0.59	1.12
15	12/01/01 13:04	0.89	2.04	0.84	1.70
16	12/03/01 16:05	1.08	1.76	0.53	0.94
17	12/04/01 10:56	1.21	1.33	0.42	0.56
18	12/04/01 19:30	1.30	1.04	0.35	0.37
19	12/05/01 16:04	1.31	1.03	0.35	0.36
20	12/06/01 05:00	1.08	1.78	0.54	0.96
21	12/08/01 12:31	1.10	1.70	0.52	0.89
22	12/12/01 22:50	1.07	1.80	0.55	1.00
23	12/13/01 04:43	1.11	1.66	0.50	0.83
24	12/13/01 09:45	1.09	1.72	0.52	0.90
25	12/13/01 16:27	0.92	2.06	0.78	1.61
26	12/16/01 18:27	1.00	2.00	0.64	1.29
27	12/17/01 02:27	0.99	2.02	0.66	1.33
28	12/18/01 15:08	1.01	1.98	0.62	1.24
29	3/5/02 02:07	1.09	1.75	0.53	0.93
30	3/8/02 14:14	1.20	1.34	0.42	0.56
31	3/9/02 22:06	1.24	1.21	0.39	0.48
32	3/10/02 14:12	1.07	1.80	0.55	1.00
33	3/26/02 09:58	1.11	1.66	0.51	0.84
34	3/27/02 13:02	1.08	1.76	0.54	0.95

It should be noted that the environmental loading factor gives only a proportional representation of the wave loading acting on the bridge and that no actual loads are calculated. However, while actual wave loads were not calculated, a rational approach was taken in developing the environmental loading factor which provides the ability to proportionally describe the magnitude of the wave loading acting on the bridge for the observed storm events, or for a general storm event with a given wind speed and direction. The environmental loading factor was coupled with the measurements of cable tension during the corresponding storm event to develop an empirical relationship that can be used to predict the mooring cable forces.

MAXIMUM CABLE TENSION PREDICTION FOR GENERAL STORM EVENT

Following the statistical analysis and development of the environmental loading factor, the 34 $T_{M\text{-}To}$ and T_{STDEV} values obtained from the cable tension measurement records were plotted versus the corresponding environmental loading factor and a best fit curve developed through the data. This was done to enable the prediction of $T_{M\text{-}To}$ and T_{STDEV} for a general storm of given magnitude. Figures 8 and 9 show representative plots of $T_{M\text{-}To}$ and T_{STDEV}, respectively, and the fitted exponential curves versus the environmental loading factor for cable A_s. Similar curve fitting was performed for each of the other instrumented cables. Plots for the other instrumented cables are provided in Appendix A. The points in Figures 8 and 9 labeled "Glosten" were obtained from the previous analysis of the EPFB (The Glosten Associates 1993a) and are included to give reference between the experimentally-obtained measurements and those determined through the previous analysis prior to retrofit of the mooring cables.

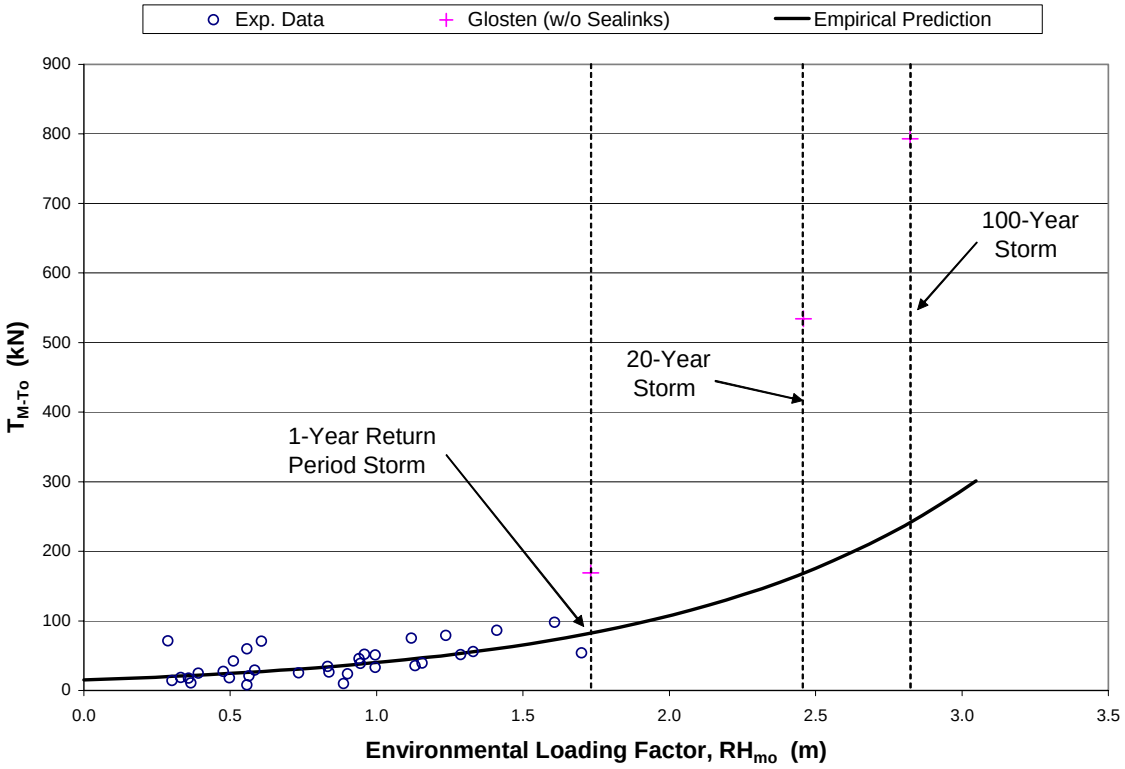

Figure 8 - T_{M-To} vs. Environmental Loading Factor, Cable A_s

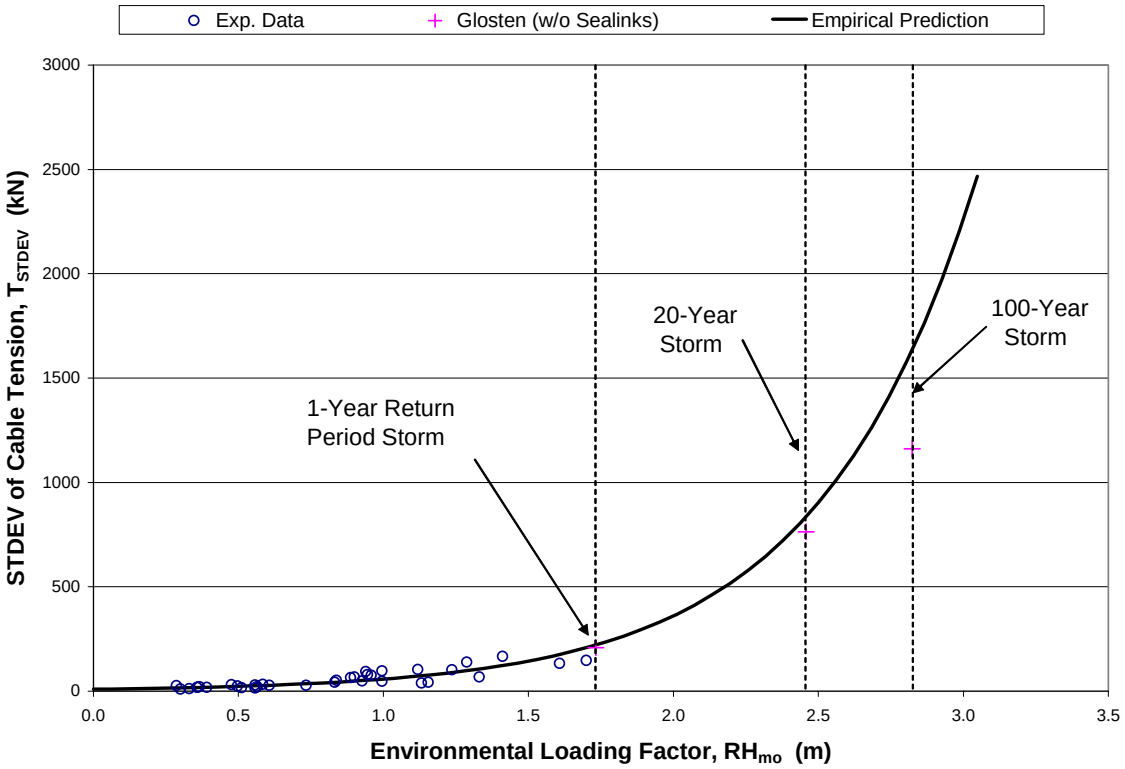

Figure 9 - T_{STDEV} vs. Environmental Loading Factor, Cable A_s

Equation 2 may be rewritten expressing $T_{M\text{-}To}$ and T_{STDEV} as a function of the environmental loading factor. The expression for the predicted maximum cable tension corresponding to a given level of confidence for a general storm is shown in Equation 5 and the terms $T_{M\text{-}To}$ and T_{STDEV} are calculated according to Equations 6 and 7, respectively.

$$T^{p}_{\max} = T_o + \left[T^{p}_{M-To}(ELF) + G_F T^{p}_{STDEV}(ELF)\right] \quad \text{(Equation 5)}$$

$$T^{p}_{M-To}(ELF) = Ae^{k(ELF)} \quad \text{(Equation 6)}$$

$$T^{p}_{STDEV}(ELF) = Be^{m(ELF)} \quad \text{(Equation 7)}$$

In Equation 5, the term ELF denotes the environmental loading factor, and in Equations 6 and 7 the terms A, k, B, and m are coefficients determined through the curve fitting of the exponential curves to the experimental data. $T^{p}_{M\text{-}To}$ and T^{p}_{STDEV} are expressed with the superscript p to indicate that the values are predicted through the exponential curves fit to the data rather than evaluated from the experimental records. Specific values for the coefficients are listed in Table 6 for the calculation of $T_{M\text{-}To}$ and T_{STDEV}, respectively, for the instrumented cables.

The R^2 values listed in Table 6 are included as a measure of how well the exponential curves fit the experimental data, where $R^2 = 1.0$ represents a perfect fit. Note that the R^2 values in Table 6 for the $T_{M\text{-}To}$ prediction curves are not considered good from a statistical standpoint, possibly due to the wide range of variation in cable pretension during the months while the bridge was being monitored. In contrast, the R^2 values for the T_{STDEV} prediction curves indicate a good statistical fit.

Table 6 – Coefficient Values for T_{M-To} and T_{STDEV} Predictions

Cable	T_{M-To}			T_{STDEV}		
	B (kN)	k	R^2	A (kN)	c	R^2
A_s	14.916	0.986	0.34	9.215	1.834	0.79
B_s	12.441	1.231	0.47	3.125	1.709	0.74
C_s	13.291	1.232	0.45	4.877	1.384	0.83
I_s	5.615	1.456	0.38	2.869	1.546	0.84
R_s	5.667	1.296	0.26	2.452	1.791	0.89
Y_s	12.066	1.333	0.38	4.192	1.465	0.87
Z_s	10.833	1.330	0.38	3.652	1.825	0.83
AA_s	7.993	1.257	0.25	6.202	1.971	0.82

A climatological analysis, performed as part of a previous analytical study for the EPFB, determined that the 1-year storm event corresponded to a 1-minute average wind speed of 76 km/hr, wave height H_{mo} = 0.85 m, and wave period T_m = 3.23 seconds (The Glosten Associates 1991a, 1993a). Using the reported parameters for the waves corresponding to the 1-year storm, the environmental loading factor was calculated as ELF = 1.7 m. It should be noted that the experimental data points shown in Figures 8 and 9 represent storms at or below the 1-year return period magnitude. It follows that the ability to predict the maximum cable tension values from the empirical relationships developed is limited by the magnitude of the storm events that occurred over the 2001-2002 winter season. Extension of the empirical prediction curves to 20-year and 100-year return period storm events requires significant extrapolation beyond the collected data such that the predictions are considered unreliable. This extension of the exponential curves is shown in Figures 8 and 9 as well as in Figures A.1 through A.14 to illustrate the extent of extrapolation required beyond the collected data for the 20-year and 100-year storms. However, an evaluation of the effectiveness of the elastomers and

the overall distribution of cable forces among mooring cables can be made from the 1-year storm events. This evaluation will be discussed in the section entitled Findings and Discussion.

ANALYSIS OF RETROFITTED EPFB MOORING CABLES

In addition to the measurement of cable forces on the bridge, the retrofitted mooring cables were also evaluated analytically. A method of cable analysis given by Ahmadi-Kashani and Bell (1988) was modified for the analysis of the 70 mm diameter mooring cables with two elastomers. Development of the analysis technique used to model the retrofitted mooring cables is given in Peterson (2002).

A structural model of the retrofitted cables was constructed as shown in Figure 10. The cable was modeled using the technique developed by Ahmadi-Kashani and Bell (1988), while the Sealink elastomers were modeled as nonlinear elements using information obtained from load-extension tests performed on the Sealinks (Lehigh Univ. 1993). In Figure 10, L_s denotes the unstretched length of the Sealinks and L'_{so} denotes the stretched length of the Sealinks under the specified cable pretension, T_o. The submerged unit weight of the cable, q_o, was considered in the development of the analysis procedure presented by Ahmadi-Kashani and Bell (1988), and the submerged weight of the Sealinks, w_S, was lumped and applied at nodes B and C.

The analysis of the mooring cables was accomplished by assigning horizontal displacements to the pontoon to which the mooring cable under consideration was connected, denoted as node P, while assuming the cable anchor, node A, to be rigidly fixed to the lake bottom. For a given horizontal displacement of the pontoon, the positions of nodes B and C were adjusted iteratively such that force equilibrium was

obtained at each of the nodes. Force equilibrium was assigned when the internal forces in the cable and Sealink elastomers at nodes B and C closely matched (within a given tolerance) the external loading applied at the nodes.

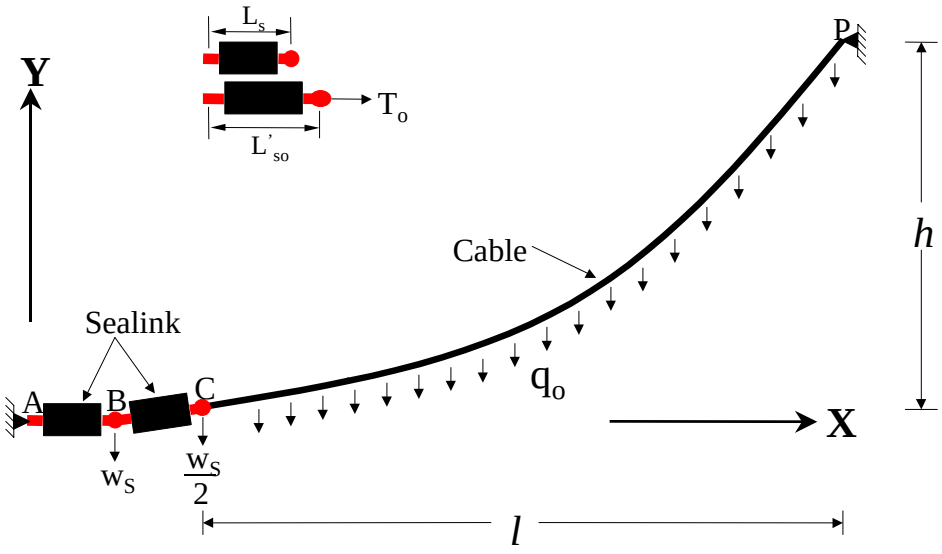

Figure 10 – Structural Model of Mooring Cable and Sealinks

The analysis was performed to obtain relationships between the cable tension versus horizontal pontoon displacement and between cable stiffness and horizontal pontoon displacement. Figure 11 shows plots of the tension-displacement and the stiffness-displacement relationships for cable A_s. Similar plots for the other retrofitted mooring cables are provided in Appendix B. A positive displacement in the analysis was a displacement of the pontoon to the north while negative displacements were to the south.

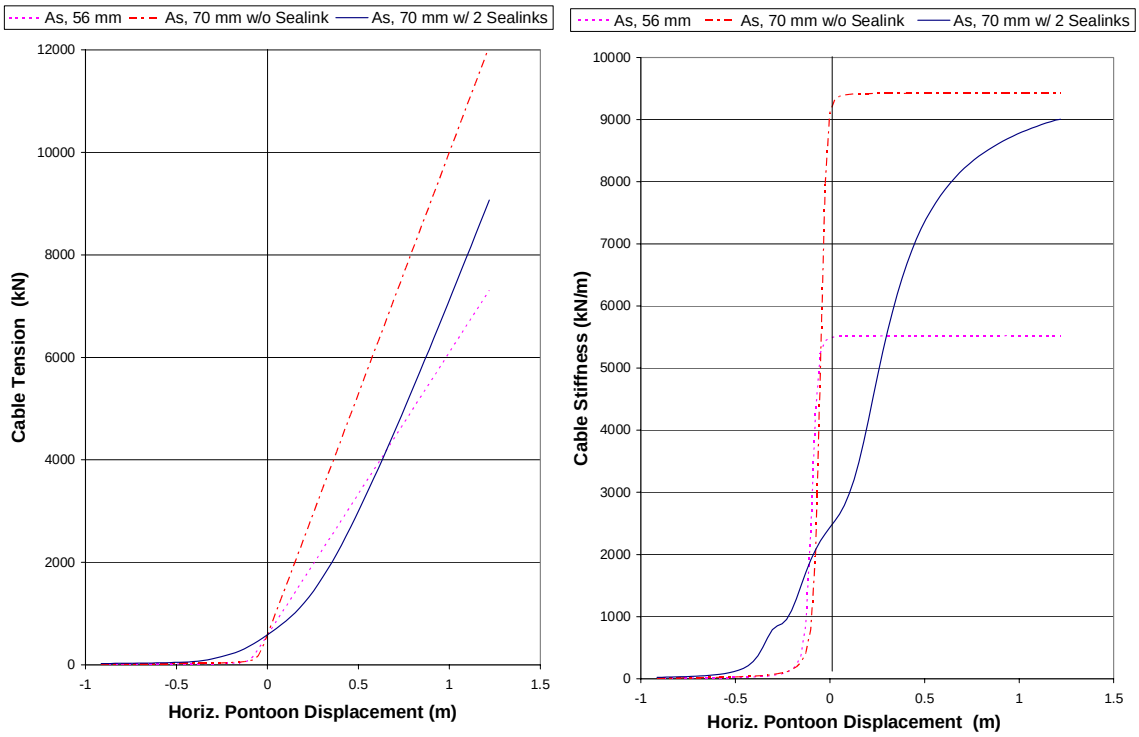

Figure 11 - Cable Tension (left) and Cable Stiffness (right) vs. Horizontal Pontoon Displacement

Finally, two FORTRAN programs were written to analyze the mooring cables both with and without Sealink elastomers. Listings of these programs are given in Peterson (2002) and may also be obtained by contacting the authors. The program written for the analysis of the retrofitted mooring cables may be used to consider any number of Sealink elastomers connected in series with the mooring cable.

EPFB PARAMETRIC STUDY

Following the development of the analysis technique used to analyze the retrofitted mooring cables, a computer model was developed to represent the bridge. The computer model was used to perform a parametric study considering the effects on the structural response of the floating bridge due to several changes to the configuration of

the mooring system, including the addition of more than two Sealink elastomers to the retrofitted cables and several changes to the pretension values at various mooring cables. Each of the analysis cases were used to investigate changes to the bridge which may result in improved performance for the floating bridge. The main structural response of interest in the parametric study was the response of each of the mooring cables since the mooring system performance was the primary focus of the study. However, sway displacements and lateral bending moments were also considered throughout the parametric study since it was necessary to determine if changes to the mooring system which resulted in improvements to the performance of the cables might also result in negative effects elsewhere in the structure.

The computer model was constructed using the cable analysis method developed to represent each of the mooring cables, and beam elements were used to represent the pontoons. Only sway displacements and yaw rotations were considered since these motions were the main contributors to the forces in the mooring cables, the performance of which was the main focus of the study. Material stiffness and section property values developed previously were used in the computer model: E = 27.8 GPa and the section property values as calculated by KPFF Engineers and reported by The Glosten Associates (1993b).

Finally, the loading considered was the slowly-varying loads from wind and wave drift forces corresponding to the 100-year storm event. The dynamic wave forces were not considered since the parametric study was considered as a first-step in the investigation of several possible changes to the mooring system configuration that may improve the performance of the floating bridge. The 100-year steady wind and wave

forces were selected since the effects on the structural response due to changes in the mooring system configuration were more pronounced for the higher loading. Aerodynamic forces were calculated using the wind force coefficients previously reported (The Glosten Associates 1993b). The wave drift forces were determined through a force balance between the total environmental loading and the total horizontal cable force. The total aerodynamic force on the floating bridge (determined through the wind force coefficients) was subtracted from the total lateral resisting force to yield the total wave drift force acting on the bridge. Nodal loads were then calculated as the sum of the aerodynamic forces acting on each node and the total wave drift force uniformly distributed along the length of the EPFB.

Before proceeding with the parametric study, the original mooring system was modeled and the results were compared to those reported from the previous analysis of the EPFB (The Glosten Associates 1993a). The results obtained from the current structural model agreed well with those reported previously, and the computer model was considered sufficiently accurate to proceed with the parametric study. In addition, the analytically-determined values agreed with the experimentally-obtained cable tension values with error values between 0.24% and 14%. More detailed information on the construction of the computer model and the analysis of the floating bridge is available in Peterson (2002).

Analysis Cases

The analysis cases considered for the parametric study were collected into three groups. Group 1 analyses were performed for the mooring system in the pre-retrofit, post-retrofit, and post-retrofit configuration without Sealink elastomers added to the 70

mm diameter cables A_s, B_s, Z_s, and AA_s. For each of the three analyses, the axial pretension in all of the mooring cables (except the longitudinal cables located near the drawspan) was equal to 580 kN.

For the second group of mooring system configurations considered in the parametric study, three cases were considered in which more than two Sealink elastomers were connected to the larger diameter replacement cables A_s, B_s, Z_s, and AA_s, including the addition of three, four, and six Sealinks to the larger diameter replacement cables along with. Comparisons were made with respect to the current or post-retrofit configuration.

In addition, it was also of interest to investigate changes in the pretension values at various mooring cable pairs that might improve the performance of the floating bridge more cost effectively than through the replacement of the already retrofitted cables with new differently-retrofitted cables. These may be desirable since the changes to the pretensioning configuration can be made with little or no extra cost to the WSDOT. The specific pretension configurations considered in the Group 3 analyses are listed in Table 7. Unless specified in Table 7, the pretension, T_o, of the mooring cables was taken as being 580 kN.

Table 7 – Pretension Configurations

Cable Pair	Pretension Config. 1 T_o (kN)	Pretension Config. 2 T_o (kN)	Pretension Config. 3 T_o (kN)
A	400	360	360
B	450	400	400
C	580	580	450
Y	580	580	450
Z	450	400	400
AA	400	360	360

FINDINGS AND DISCUSSION

CONCRETE STRAINS

As was discussed earlier, the strain gage readings recorded during the storm events captured could not be used to obtain absolute strain measurements because of changes in the water level and temperatures. However, the strain measurements are still of some value. Some of the strain gage measurements were used to identify one of the natural frequencies of vibration of the bridge as 0.35 Hz. In addition, the frequency content of the strain gage measurements was used as an indicator of which of the strain gages yielded meaningful information and which yielded noisy or meaningless information. The frequency analysis of the strain gage measurements is discussed further in Peterson (2002).

In addition, the magnitude of change in the signal readings recorded during the storms of winter 2001-2002 is of interest. Following the 1993 Inauguration Day Storm, the bridge was post-tensioned in the interest of closing existing cracks and in an attempt to prevent further cracking of the bridge during future storm events. Thus, the strain gage measurements were also analyzed to determine if the strains experienced during the winter storms of 2001-2002 were above or below concrete cracking strains.

In the absence of information concerning the baseline signal values for each of the strain gages, the overall change in strain during each of the individual storm events were evaluated as shown in Equation 8. $\Delta\varepsilon$ denotes the strain range or overall change in strain, and the values denoted V_{max} and V_{min} correspond to the maximum and minimum strain gage voltage readings, respectively, obtained from an individual storm record for a particular strain gage. Table 8 shows values of the strain range obtained from selected

strain gages during the larger magnitude storm events recorded over the 2001-2002 winter season.

$$\Delta\varepsilon = 1000\left(V_{\max} - V_{\min}\right) \qquad \text{(Equation 8)}$$

Table 8 – Strain Range Values

Storm Record	Strain Range, Δε				
	SG # 1 (με)	SG # 5 (με)	SG # 8 (με)	SG # 10 (με)	SG # 13 (με)
1	42	69	9	42	74
4	63	92	13	62	39
14	61	64	14	45	38
15	87	109	18	86	55
16	45	52	16	44	38
21	53	70	129	45	42
22	72	56	14	29	41
23	41	45	12	17	30
25	83	117	68	81	56
26	65	99	13	68	39
27	55	85	13	35	38
28	99	82	15	44	38
29	48	53	13	35	37
32	54	44	17	41	44
33	79	62	26	41	40
34	63	58	19	63	46

Without baseline signal values for the strain gages, some discernment must be used to interpret the strain range values shown in Table 8. For storm events 29 through 34, which occurred during March 2002, baseline values were obtained for each of the strain gages. Using these baseline values in the interpretation of the strain gage measurements, it was determined that the strain values were typically distributed relatively uniformly about the baseline signal values. Thus, in the interpretation of the strain gage measurements corresponding to the storm events captured during the winter months, it was assumed that these measurements were also uniformly distributed about

the unknown baseline values. Using this assumption, the strain range values listed in Table 8 were interpreted as twice the maximum positive and negative strains.

Approximately 2.7 MPa of compressive stress was added to the pontoons through the post-tensioning work performed on the bridge (Johnson and Brallier 2000). The compressive stress induced by the post-tensioning of the pontoons was calculated as approximately 60 με. Thus, the concrete in the pontoons must experience tensile strains of approximately 160 με as measured by the strain gages before cracking can occur. This is true since the strain gages were installed on the concrete while the pontoons were pre-compressed by approximately 60 με, and this pre-compressive strain must be added to the tensile strain limit of 100 με to obtain the cracking strain under the post-tensioning (MacGregor 1997).

By comparing the strain range values listed in Table 8 to the strain required to reach cracking in the concrete, it can be concluded that the strains measured in pontoon R are well below the cracking limit of the concrete. Specifically, this evaluation was made by calculating the maximum positive strains as one-half the strain range values listed in Table 8 and comparing these strains with an assumed cracking strain of 160 με.

MOORING CABLE TENSION

From the cable tension measurements, four natural frequencies of vibration were identified for the bridge. The average values of the natural frequencies identified from the cable tension measurements for each of the storm records are listed in Table 9 along with the natural frequency identified through the strain gage measurements. Frequencies f_1 and f_4 are the main frequencies of interest, since f_1 is close to the wind frequency and f_4 is close to the calculated wave frequency for each of the recorded storm events. In

addition to the natural frequencies of vibration, the damping ratio for the floating bridge was determined to be approximately $\xi = 0.25$, or 25%, through an analysis of the apparent amplification of cable tension versus wave forcing frequency. Further details concerning the determination of the natural frequencies of vibration and approximate damping ratio for the bridge are provided in Peterson (2002).

Table 9 – EPFB Natural Frequencies of Vibration

Natural Frequency f_n	Cable Tension Data (Hz)	Strain Gage Data (Hz)
f_1	0.03	
f_2	0.12	
f_3	0.22	
f_4	0.36	0.34

The cable tension measurements were also used to evaluate the effectiveness of the Sealink elastomers in improving the performance of the mooring system. Since no experimental measurements of cable tension were made prior to the replacement of the cables, the maximum cable tension values prior to retrofit were obtained from the earlier analytical study of the EPFB (The Glosten Associates 1993a). The empirically-predicted values of maximum cable tension were calculated for a 90% confidence level using the previously determined environmental loading factor for the 1-year storm event (ELF = 1.7 m) and compared to the maximum (90% confidence) cable tension values obtained from the previous analysis. The empirically-determined values based on experimental measurements and those corresponding to the previous analysis are listed in Table 10 for comparison.

It should be noted that two simultaneous comparisons are required to evaluate the effectiveness of the elastomers on the basis of comparisons between the experimentally-determined maximum cable tension values with those from the previous analysis. These comparisons are the comparison between experiment and analysis and the comparison between pre-retrofit behavior with that after the mooring cables were retrofitted with Sealinks. Thus, an evaluation of the performance of the Sealink elastomers cannot be made entirely from an experimental perspective, but rather by combining the experimental measurements with additional information provided from the analysis of the retrofitted mooring cables performed as a part of this study.

Table 10 – Max. Cable Tension Values Before & After Retrofit, 1-Year Loading

EPFB Mooring Cable	Analysis T^{A}_{max} (Pre-Retrofit) (kN)	Experimental T^{E}_{max} (Post-Retrofit) (kN)	T^{E}_{max}/T^{A}_{max}	Normalized T^{A}_{max}	Normalized T^{E}_{max}
A_s	1674	1519	0.91	1.87	1.79
B_s	1348	920	0.68	1.51	1.08
C_s	1031	901	0.87	1.15	1.06
I_s	908	812	0.89	1.02	0.96
R_s	894	848	0.95	1.00	1.00
Y_s	989	908	0.92	1.11	1.07
Z_s	1108	1025	0.92	1.24	1.21
AA_s	1302	1392	1.07	1.46	1.64

Inspection of Table 10 shows that the experimentally-determined maximum cable tension values are lower than those from analysis for the pre-retrofit configuration by 5% to 32%, except at cable AA_s. It may be noted that the highest apparent reduction in cable tension was at cable B_s, while the cables away from the ends of the bridge (C_s, I_s, R_s, and

Y_s) tend to show less reduction. This may be expected since changes to the mooring system were made only at the ends of the bridge.

The cable retrofit was intended to reduce the load attraction at the shorter and stiffer mooring cables. The columns labeled "Normalized" in Table 10 correspond to T_{max} values normalized at each of the instrumented cables with respect to the T_{max} value for cable R_s. The cable tension value at cable A_s is 79% higher than the tension at cable R_s, and the tension at cable AA_s is 64% higher than that at cable R_s. However, the analytical results corresponding to the pre-retrofit configuration show tension values at cable A_s 87% higher than at cable R_s.

While the maximum cable tension values based on experimental measurements were calculated using the environmental loading factor, prediction curves were plotted with respect to peak wind speed to make the interpretation more intuitive. It should be noted that a 1-year storm event corresponds to peak or gust wind speeds approximately equal to 95 km/h. Figure 12 shows that the peak cable tension values for a 1-year event at cables A_s and AA_s are significantly higher than for the other instrumented cables shown. Also, the plotted prediction curves show that the tension values at cables B_s and Z_s are more on the order of the longer cables (cables C_s, I_s, R_s, and Y_s).

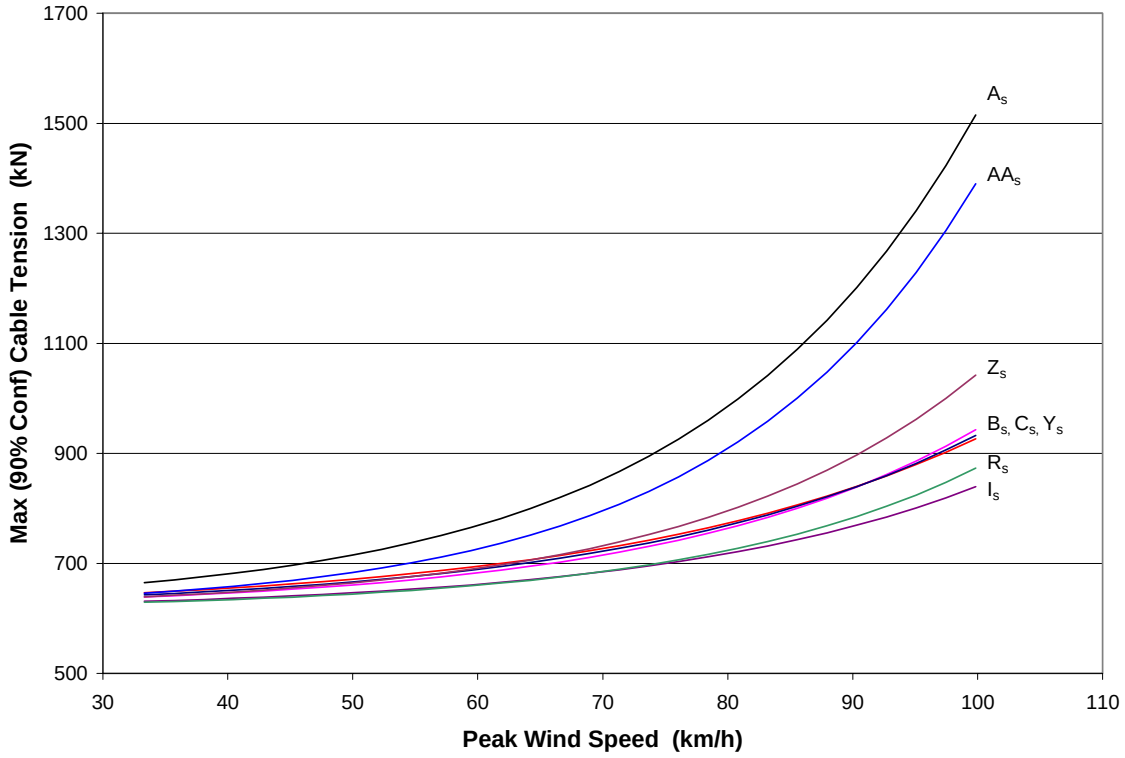

Figure 12 – Predicted Max Cable Tension vs. Peak Wind Speed

EPFB MOORING CABLE ANALYSIS

Figure 13 plots calculated stiffness values for the mooring cables before and after retrofitting. Inspection of the figure shows that the larger 70 mm diameter replacement cables retrofitted with the elastomers are more flexible than the previous 56 mm diameter cables for pontoon displacements 0.3 m to the north or less. Based on the results of the previous EPFB analysis (The Glosten Associates 1993a), this smaller displacement is approximately the total displacement of the end pontoons during the 1-year storm event. It is also noted in Figure 13 that, as the horizontal pontoon displacements increase above 0.3 m, the retrofitted cables are expected to have a higher stiffness value than the original 56 mm diameter cables. This leads to the conclusion that, during the 20-year and 100-

year storm events, the retrofitted cables may behave stiffer, resulting in the attraction of higher loads than would have been experienced prior to retrofit.

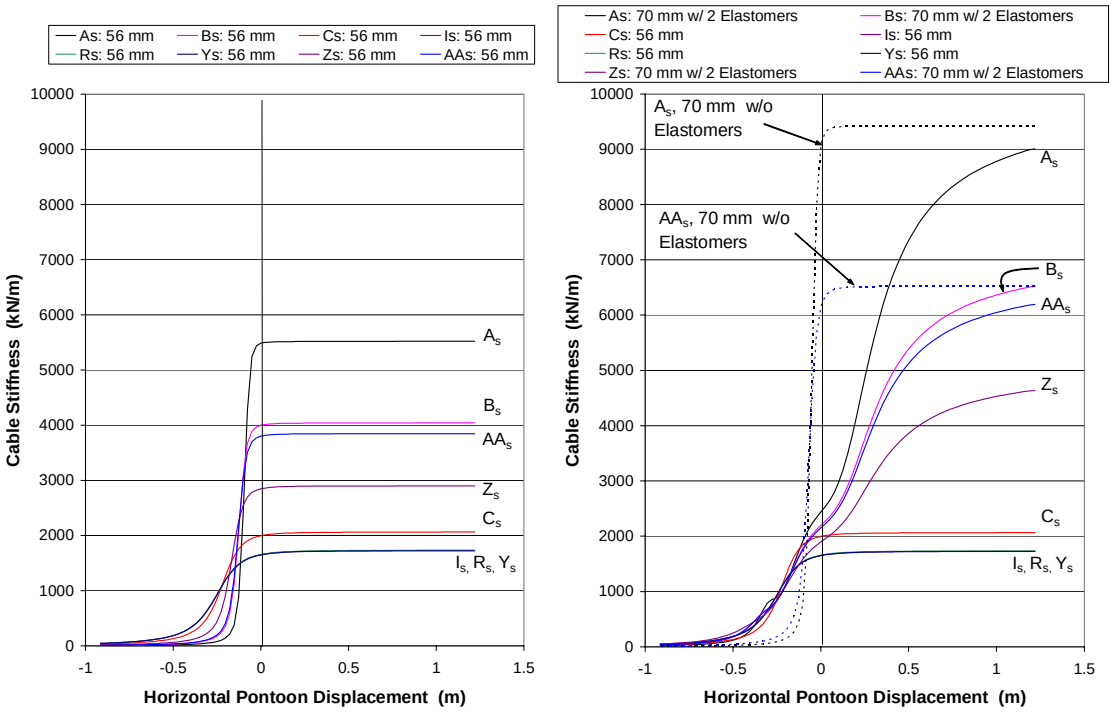

Figure 13 - Cable Stiffness vs. Horizontal Pontoon Displacement, Before (left) & After Retrofit (right)

The stiffness versus displacement plot for the post-retrofit configuration (right) shows curves representing the larger diameter replacement cables A_s and AA_s without the addition of elastomers. Comparison between the curves corresponding to cables A_s and AA_s with and without elastomers shows that the retrofitted cables are significantly more flexible with the elastomers than without. Thus the addition of elastomers was effective in reducing the stiffness of the retrofitted cables. However, for larger pontoon displacements, the use of larger diameter cables over rides the stiffness reduction due to the elastomers resulting in retrofitted end cables that act stiffer than the cables that were

replaced. The stiffness versus displacement curves for cables C_s, I_s, R_s, and Y_s are also shown in Figure 13 to illustrate the different stiffness values of the other mooring cables located along the length of the bridge.

EPFB PARAMETRIC STUDY

Group 1 Analyses

Group 1 analyses were performed for the EPFB mooring system in the pre-retrofit, post-retrofit and post-retrofit configuration without Sealink elastomers. Tabulated results for the parametric study are included in Table 11 and are expressed as percent differences between responses for the analysis cases considered. The percent differences between the structural response quantities for the particular analysis cases considered are labeled in the heading above the columns of the table as, for example, 1B & 1A. The percent difference values are calculated according to Equation 9 where the first analysis case listed in the column heading is taken as the "test" value and the second listed is taken as the "reference" value for the percent difference calculation. Thus, a positive percent difference value indicates an increase in value of the structural response for the test analysis with respect to the reference analysis, while a negative value indicates a decrease in value of the structural response considered.

$$\%Diff = 100\left[\frac{test - ref}{ref}\right] \qquad \text{(Equation 9)}$$

Comparison of the structural responses shown in Table 11 between the pre-retrofit and post-retrofit mooring system configurations (1B & 1A) was made to analytically quantify the changes in structural response under steady wind and wave loading with respect to the original configuration of the mooring system. It was already noted through

experimental measurements of cable tension at the retrofitted cables that these cables continue to attract loads significantly higher than at cables located away from the ends of the floating bridge. However, the question still remains concerning what improvement was obtained through the retrofit of the replacement cables with Sealink elastomers.

Table 11 - Tabulated Results for Parametric Study, Group 1

Pontoon/ S. Cable	Cable Tension		Sway Displacement		Lateral Bending Moment	
	% Diff 1B & 1A	% Diff 1C & 1A	% Diff 1B & 1A	% Diff 1C & 1A	% Diff 1B & 1A	% Diff 1C & 1A
A	-7.74	-3.19	44.15	-44.27	-3.13	-14.10
B	-3.53	19.74	20.46	-23.08	-7.06	-3.43
C	4.21	-5.83	6.96	-9.66	13.17	-26.25
D	1.32	-2.49	2.24	-4.22	-10.43	6.86
E	0.18	-0.96	0.31	-1.64	-15.92	15.47
I	-0.30	0.35	-0.61	0.72	-1.29	2.01
R	-0.06	0.12	-0.12	0.24	-0.01	-0.29
W	0.17	-0.81	0.28	-1.35	-6.70	6.97
X	0.90	-1.99	1.52	-3.34	4.33	1.26
Y	2.42	-3.99	4.42	-7.27	-4.47	1.69
Z	-3.82	20.77	13.63	-17.74	-2.57	-6.58
AA	-4.86	0.58	35.38	-39.59	0.54	-22.55

Analysis 1A = Pre-Retrofit Mooring System Configuration
Analysis 1B = Post-Retrofit Mooring System Configuration
Analysis 1C = Post-Retrofit Mooring System Configuration w/o Sealinks

Inspection of the percent difference values listed in Table 11 between the cable tension values for analysis cases 1B & 1A shows that the cable tension decreased at the cables retrofitted with Sealink elastomers, and a small increase in cable tension was noted for the cables immediately adjacent to the retrofitted cables, cables C_s and Y_s. When comparing the sway displacements, Table 11 shows an increase in sway displacement at the ends of the floating bridge when comparing analysis cases 1B & 1A. Finally,

comparison of the maximum lateral bending moments for analysis cases 1B & 1A shows a general decrease away from the midspan.

Group 2 Analyses

Group 2 analyses considered the addition of two, three, four and six Sealink elastomers to the retrofitted mooring cables. Group 2 results are summarized in Table 12.

Table 12 - Tabulated Results for Parametric Study, Group 2

Pontoon/ S. Cable	Cable Tension			Sway Displacement			Lateral Bending Moment		
	% Diff 2A & 2B	% Diff 2A & 2C	% Diff 2A & 2D	% Diff 2A & 2B	% Diff 2A & 2C	% Diff 2A & 2D	% Diff 2A & 2B	% Diff 2A & 2C	% Diff 2A & 2D
A	-2.09	-3.92	-7.31	28.91	56.89	109.42	2.56	3.46	2.47
B	-7.56	-13.13	-20.75	16.73	32.74	62.49	-3.52	-7.90	-17.76
C	4.33	8.39	15.80	6.98	13.52	25.46	14.44	27.31	49.65
D	1.62	3.09	5.69	2.72	5.19	9.57	-9.61	-19.22	-37.81
E	0.43	0.79	1.36	0.74	1.36	2.33	-17.61	-34.68	-66.79
I	-0.30	-0.58	-1.11	-0.61	-1.19	-2.26	-1.47	-2.83	-5.26
R	-0.08	-0.14	-0.26	-0.16	-0.30	-0.54	0.01	-0.01	-0.06
W	0.25	0.45	0.75	0.43	0.75	1.26	-8.19	-16.09	-30.38
X	1.13	2.13	3.87	1.89	3.58	6.47	4.17	8.62	17.15
Y	2.85	5.49	10.14	5.10	9.81	18.12	-5.03	-10.12	-19.62
Z	-5.89	-10.05	-15.74	14.04	27.33	51.12	-2.11	-4.92	-10.92
AA	-0.06	-0.39	-1.77	30.12	59.00	111.15	2.61	3.32	2.45

Analysis 2A = Post-Retrofit Mooring System Configuration
Analysis 2B = Replacement Cables w/ 3 Sealinks
Analysis 2C = Replacement Cables w/ 4 Sealinks
Analysis 2D = Replacement Cables w/ 6 Sealinks

Inspection of Table 12 shows that the addition of an increasing number of Sealink elastomers to cables A_s, B_s, Z_s, and AA_s results in a progressive reduction in the tension values at the retrofitted cables. However, the parametric study also shows that as the cable tension values are progressively reduced at the retrofitted cables, the response of the floating bridge shifts such that load is shed to the mooring cables adjacent to those retrofitted with Sealinks. This results in an increase in tension at cables C_s and Y_s for the

configuration in which six Sealinks are considered. Thus, the parametric study shows that a true uniform distribution of steady wind and wave loading cannot be obtained along the length of the bridge by adding Sealink elastomers.

In addition, the parametric study for Group 2 shows that the addition of more Sealink elastomers may lead to significant increases in sway displacements and moderate reductions in lateral bending moments.

Group 3 Analyses

Group 3 analyses investigated the effects of changes in the pretension values of the mooring cables on bridge response. Group 3 results are summarized in Table 13.

Table 13 - Tabulated Results for Parametric Study, Group 3

Pontoon/ S. Cable	Cable Tension			Sway Disp.			Lateral Bending Moment		
	% Diff 3A & 3B	% Diff 3A & 3C	% Diff 3A & 3D	% Diff 3A & 3B	% Diff 3A & 3C	% Diff 3A & 3D	% Diff 3A & 3B	% Diff 3A & 3C	% Diff 3A & 3D
A	-7.62	-8.43	-7.18	25.11	33.59	35.20	-0.19	0.18	1.90
B	-5.58	-7.57	-5.56	14.23	19.09	21.40	-4.62	-5.89	-0.53
C	3.54	4.78	-2.75	5.71	7.70	10.44	11.01	14.99	5.45
D	1.24	1.69	3.06	2.09	2.85	5.14	-8.92	-11.82	-6.02
E	0.27	0.38	1.34	0.46	0.65	2.30	-15.39	-20.57	-18.58
I	-0.25	-0.34	-0.38	-0.51	-0.69	-0.78	-1.17	-1.59	-2.43
R	-0.12	-0.16	-0.24	-0.25	-0.33	-0.49	-0.16	-0.20	0.31
W	0.21	0.30	1.33	0.35	0.51	2.24	-13.73	-18.12	-16.88
X	1.54	2.07	3.65	2.58	3.46	6.11	8.86	11.50	1.60
Y	4.29	5.72	-3.14	7.67	10.22	13.77	-9.47	-12.40	-6.49
Z	-4.63	-6.49	-3.98	22.45	29.76	33.88	-6.72	-8.56	-2.54
AA	-5.02	-5.51	-3.43	49.73	65.75	70.55	-2.92	-3.16	-0.01

Analysis 3A = Post-Retrofit Mooring System Configuration
Analysis 3B = Pretension Configuration 1
Analysis 3C = Pretension Configuration 2
Analysis 3D = Pretension Configuration 3

The results of the parametric study considering changes to the pretension values at various mooring cables shows that the best improvement in floating bridge performance

may be achieved for changes made according to pretension configuration 2 as listed in Table 13. The changes in pretension values show a reduction in mooring cable tension for the retrofitted mooring cables with an increase in cable tension at cables C_s and Y_s. These percent increase or decrease values were calculated with the current mooring system configuration used as the reference, and are of the same magnitude or slightly better than the improvements obtained by retrofitting the replacement cables with the two Sealink elastomers. Thus, an additional improvement in performance of the floating bridge (in terms of cable tension only) above the improvements gained by adding the retrofitted mooring cables may be obtained by simply setting the pretension values according to those set for the pretension configuration 2 analysis.

However, the other structural responses should be compared as well so that improvements to the mooring cable tension values are not sought while undesirable effects are incurred elsewhere in the structure. The parametric study also showed increases in sway displacements at the ends of the floating bridge for pretension configuration 2. In addition, comparison of the lateral bending moment values for the analysis corresponding to pretension configuration 2 shows that the bending moments are generally reduced away from the ends of the bridge.

SUMMARY AND CONCLUSIONS

Following the structural damage to the Evergreen Point Floating Bridge (EPFB) caused by the 1993 Inauguration Day Storm, several retrofit measures were undertaken to strengthen the bridge to withstand future storm events. Larger-diameter replacement mooring cables were installed near the ends of the bridge (cables A_s, B_s, Z_s, and AA_s) and included Sealink elastomers in order to provide energy dissipation and increased cable flexibility in the shorter end cables and allowing a more even distribution of mooring cable tension among the cables during storm events. Following the installation of the retrofitted mooring cables, the Washington State Department of Transportation (WSDOT) issued a contract to Washington State University (WSU) researchers to determine the effectiveness of the Sealink elastomers in reducing the over-stiff effects of the shorter mooring cables on the bridge and to evaluate the distribution of wind and wave loading to the mooring cables along the length of the floating bridge.

Experimental measurements of wind speed and direction and cable tension were obtained during 34 storm events during the winter season of 2001-2002. It was determined that the recorded storm events generally fell below the 1-year return period storm, while a few of the events were approximately equal in magnitude to the 1-year event. Following the collection of cable tension measurements, statistical analysis of the data was performed that enabled the use of physically meaningful cable response parameters and resulted in an ability to predict the measured maximum cable tension values within a reasonable margin of conservatism. Using wind speed and structural response measurements as well as techniques developed by the U.S. Army Corps of Engineers for the forecasting of wind generated waves, an environmental loading factor

was developed and used to empirically predict the maximum cable tension values at each of the instrumented cables for a general storm of given magnitude.

In addition to the experimental work conducted for the current research, two analytical tasks were also performed. First, an analytical technique was developed for the analysis of the replacement mooring cables retrofitted with Sealink elastomers. The ability to analyze these retrofitted mooring cables over a range of reasonable pontoon displacements provided an understanding of the behavior of the retrofitted cables and aided in the evaluation of the effectiveness of the retrofitted cables. Second, an analytical model was developed of a full floating bridge under steady wind and wave loading and used to perform a parametric study to investigate the effects of changes to the mooring system on the overall structural response to steady wind and wave loading.

PERFORMANCE OF SEALINK ELASTOMERS

Experimental measurements showed that the load attraction issues associated with the shorter mooring cables continue to exist. The measurements provide evidence of some overall improvement, on the order of 5% and 32% reduction in cable tension when compared to analytically-obtained values prior to retrofit (The Glosten Associates 1993a). However, two simultaneous comparisons are required to make this assessment (analysis vs. experiment and pre-retrofit vs. post-retrofit) since no experimental measurements of cable tension were made prior to the replacement of cables A_s, B_s, Z_s, and AA_s. Thus, evaluation of the effectiveness of the Sealink elastomers in relieving the stiffness of the retrofitted cables cannot be made solely from an experimental perspective.

The analytical work presented comparing the behavior of the original cables with that of the replacement cables with and without Sealinks showed that the replacement 70-

mm diameter cables retrofitted with two Sealinks behave more flexibly than the original 56-mm diameter cables up to pontoon displacements of approximately 0.3 m. Further, the cable tension expected for the retrofitted cables is less than that expected for the original cables up to pontoon displacements of approximately 0.7 m. However, beyond these pontoon displacements, analyses indicate that the retrofitted cables will behave stiffer and experience higher tension loads than the original cables. Pontoon displacements predicted through the previous analysis of the bridge show that the total displacements at the end pontoons are approximately 0.6 m to 0.7 m during a 20-year storm event. Thus, based on the results of the cable analysis and the displacements predicted through the previous analytical work, the shorter mooring cables located near the ends of the floating bridge may continue to display over-stiff behavior and attract higher tension loads for 20-year and larger magnitude storm events.

Given that the original cables were damaged in past storms and could not be replaced with 56 mm diameter cables retrofitted with Sealink elastomers, comparison between the behavior of the larger-diameter cables with and without Sealink elastomers was also made. The analysis results show that the addition of two Sealinks to the replacement cables made a significant reduction in both the cable tension values and the stiffness with respect to tension and stiffness behavior of the 70-mm diameter cables without Sealinks. Thus, it may be concluded that the Sealink elastomers were successful in improving the behavior of the retrofitted cables, though not to the degree desired when the replacement cables were designed.

In addition to the evaluation of the effectiveness of the Sealinks in relieving the stiffness of the shorter mooring cables, the retrofitted cables were also installed with the

intent of obtaining a more even distribution of the wind and wave loads to the mooring cables located along the length of the bridge. The distribution of environmental loading to the mooring cables was evaluated through a comparison of empirically-predicted maximum cable tension values for the 1-year storm event. The comparison showed that the end cables continue to attract between 64% and 79% higher tension loads than the cables located near the midspan of the floating bridge. The only improvement in the distribution of environmental loading to the mooring cables was noted at cable B_s based on a comparison between experimental measurements and the previous analysis results. Thus, the experimental measurements showed that a more even distribution of wind and wave loading to the mooring cables was not obtained through the installation of the retrofitted mooring cables.

DESIRED EPFB PERFORMANCE

A parametric study was conducted as a first step in investigating various changes that may be made to the mooring system such that improved performance of the floating bridge may be obtained. Parameters investigated included the effects on structural response of the installation of more than two Sealink elastomers at the retrofitted cables and the effects of changes in the pretension values at various mooring cable pairs.

Analysis results showed that a true uniform distribution of steady wind and wave loading could not be obtained along the length of the bridge by adding additional Sealink elastomers. Changes to the pretension values at various mooring cables may result in additional improvements on the same order as the improvements obtained through the installation of the retrofitted mooring cables, producing an approximate reduction in cable tension of 8%. The analyses also showed increases in sway displacements at the

ends of the floating bridge of up to 66% and a general reduction in lateral bending moments by up to 20%. Thus, if the increased sway displacements at the ends of the floating bridge may be permitted, then changing the pretension values at various mooring cable pairs may lead to additional improvements in the performance of the bridge response with little or no additional cost to the WSDOT.

In addition, strain measurements obtained in this study showed that the concrete pontoons experience strains well below the cracking strains for the 1-year storm events observed during the 2001-2002 winter season. Thus, it may be concluded that the post-tensioning work conducted on the bridge following the January 1993 storm event was effective as far as can be verified through the strain gage measurements obtained through this study.

APPLICATION AND IMPLEMENTATION

MOORING SYSTEM PERFORMANCE

The experimental measurements and analytical work presented considering the behavior of the retrofitted mooring cables were performed primarily in the interest of assessing the performance of Sealink elastomers on the cables. The Sealinks were effective at reducing cable stiffness and at lessening the cable forces at the shorter end cables. However, larger cable forces continue to exist at the end cables even with the addition of the Sealinks. Analyses showed improved performance with increasing number of Sealinks, but with incremental improvements diminish as the number of Sealinks is increased. The analyses showed that it was not possible to achieve a uniform distribution of mooring cable forces along the length of the bridge through the use of Sealinks.

The analytical parametric study showed that additional improvements in the mooring system might be obtained by adjusting the pretension values at various mooring cable pairs. However, the analyses were conducted with a simplified bridge and wave loading model, and a thorough investigation and recommendations for implementation of the possible methods to improve the performance of the floating bridge were beyond the scope of this study. Additional research is needed to consider similar analysis cases with dynamic wave loading acting on the floating bridge as well as interpretation and decision making as to whether the increased sway displacements are permissible at the ends of the bridge.

FLOATING BRIDGE AND MOORING CABLE BEHAVIOR

Through various elements of the current study, comparisons were made between details of the analytical techniques used in the previous analyses of the WSDOT floating bridges and the experimental or the analytical work performed for this study. Various details within the current analysis and design methodologies used for floating bridges were confirmed or identified as needing improvements.

In terms of the statistical assumptions involved in combining the responses of a floating bridge to wind and wave loading, the experimental measurements obtained from the EPFB showed that the response process is Gaussian distributed as has previously been assumed. Further, it was noted through the experimental measurements that the predicted cable tension values for a 1-year storm event corresponding to the pre-retrofit configuration of the EPFB mooring system (The Glosten Associates1993a) are reasonably consistent with measurements made of the retrofitted mooring cables.

The perturbation analysis considered previously to determine the response of the floating bridge to dynamic wave loading is based on the assumption that the variations in bridge motion are small about the displaced configuration determined through the steady loading analysis. However, the variations in bridge sway displacements reported for the larger magnitude storms were on the order of 2 to 3.5 ft. The cable analyses conducted in this study showed that all EPFB mooring cables change dramatically in stiffness for pontoon displacements of this magnitude. Since the stiffness matrix must be linearized to perform the perturbation analysis in the frequency domain, the analysis may not yield good results for the larger magnitude dynamic wave loading.

Seemingly small changes in the diameter of mooring cables may be associated with disproportionate changes in the mooring cable behavior. This was true for the replacement of the 56-mm diameter cables with 70-mm diameter cables on the EPFB. While the change in diameter of the cables was relatively small, and it was assumed that the behavior was not significantly different between the two cable sections (The Glosten Associates 1997), analytical work presented in this study showed that the 70 mm diameter cables are approximately 70% stiffer than the former 56 mm diameter cables.

It is recommended that the full nonlinear behavior of the mooring cables be accounted for in an analysis of a floating structure, especially if elastomers are used to add flexibility to stiffer cables. Since all of the EPFB mooring cables displayed significant changes in cable stiffness over the range of pontoon displacements considered, the nonlinear behavior of the cables may have a large effect on the displacements of the bridge under wind and wave loading. In turn, the displacements of the floating bridge govern the tension loads experienced by the cables, and the resisting forces provided by the cables are a driver for the shear forces and bending moments in the pontoon sections.

The experimental measurements of cable tension showed that changes in the water level on Lake Washington produce significant changes in the cable pretension values. These changes in pretension may have a significant effect on the mooring cable behavior throughout the season when the larger magnitude storms are expected.

REFERENCES

Ahmadi-Kashani, K., Bell, A. J., (1988) "The Analysis of Cable Subject to Uniformly Distributed Loads." Engineering Structures, Vol. 10, No. 3, pp. 174-184, July 1988.

Costal Engineering Research Center (1984) *Shore Protection Manual.* US Army Engineer Waterways Experiment Station, US Government Printing Office, Washington, D.C. 4th Ed., 2 Vols., Chapter 3, pp 24-66.

The Glosten Associates (1991a) *Wind and Wave Loading Analysis, Lacey V. Murrow Replacement Bridge: Volume I, Part I: Methodology and Model.* Report prepared for the State of Washington Department of Transportation Bridges and Structures Division, Olympia, Washington. Consulting Agreement Y-4314, Glosten File No. 9121, December 1991.

The Glosten Associates (1993a) *Wind and Wave Load Analysis, Evergreen Point Floating Bridge: Final Report*. Report prepared for the State of Washington Department of Transportation Bridges and Structures Division, Olympia, Washington. Consulting Agreement Y-5101, Glosten File No. 9314, September 1993.

The Glosten Associates (1993b) *Wind and Wave Load Analysis, Evergreen Point Floating Bridge: Appendices*. Report prepared for the State of Washington Department of Transportation Bridges and Structures Division, Olympia, Washington. Consulting Agreement Y-5101, Glosten File No. 9314, September 1993.

The Glosten Associates (1997) Letter to Mark Anderson (WSDOT) from J. Thomas Bringloe of The Glosten Associates. Dated October 22, 1997, 3pp. with attached spreadsheet calculations.

Gloyd, C. S. (1988) "Concrete Floating Bridges." Concrete International, May 1988, pp. 17-24.

Hartz, B. J. (1981) "Dynamic Response of the Hood Canal Floating Bridge." Proceedings of the Second Specialty Conference on Dynamic Response of Structures: Experiment, Observation, Prediction and Control. Jan 15-16, 1981, Atlanta Georgia, pp. 16-28.

Hutchison, B. L. (1984) "Impulse response techniques for floating bridges and breakwaters subject to short-crested seas." Marine Technology, Vol. 21, No. 3, July 1984, pp. 270-276.

Isaacson, T., and Sarpkaya, M. (1981) *Mechanics of Wave Forces on Offshore Structures*. Van Nostrand Reinhold.

Johnson, R. K., and Brallier, P. A. (2000) “After the Storm: Repairing Seattle’s Evergreen Point Floating Bridge.” Structural Engineer, August 2000, pp. 34-39.

Langen, I., and Sigbjörnsson, R. (1980) “On Stochastic Dynamics of Floating Bridges.” Engineering Structures, Vol. 2, October 1980, pp. 209-216.

Lehigh University, Fritz Engineering Lab (1993) Pull-Test Report: 4-Inch Elastomeric Kinetic Chain Link. Test conducted and report prepared for VSE Corporation, Alexandria, VA. Nov., 1993.

Liu, Y. and Bergdahl, L. (1998) “Extreme Mooring Cable Tensions Due to Wave-Frequency Excitations.” Applied Ocean Research, Vol. 20, 1998, pp. 237-249.

Liu, Y., and Bergdahl, L. (1999) On Combination Formulae for the Extremes of Wave-Frequency and Low-Frequency Responses. Applied Ocean Research, Vol. 21, 1999, pp. 41-46.

Lwin, M. M. (1989) “Design of the Third Lake Washington Floating Bridge.” Concrete International, Feb 1989, pp. 50-53.

Lwin, M. M. (2000) *Chapter 22, Bridge Engineering Handbook*, edited by W. F. Chan and L. Duan. CRC Press LLC.

MacGregor, James G. (1997) *Reinforced Concrete: Mechanics and Design*. Third Edition, Prentice Hall, 1997.

Ochi, M. K. (1973) “On Prediction of Extreme Values.” Journal of Ship Research. Vol. 17, No. 1, pp. 29-37, March 1973.

Peterson, S. T. (2002) *Experimental Response and Analysis of the Evergreen Point Floating Bridge.* Ph.D. Dissertation, Washington State University.3

Smith, J. M. (1991) *Wind-Wave Generation on Restricted Fetches*. Coastal Engineering Research Center, Department of the Army Waterways Experiment Station.

Stoker, J. J. (1957) *Water Waves*. John Wiley & Sons, New York.

U.S. Army Engineer Waterways Experiment Station (1989) “Computer Program: NARFET – Wind-Wave Generation on Restricted Fetches.” CETN-I-4 3/89, Coastal Engineering Research Center, Vicksburg, Mississippi, 1989.

APPENDIX A

EMPIRICAL CURVE-FITTED PLOTS

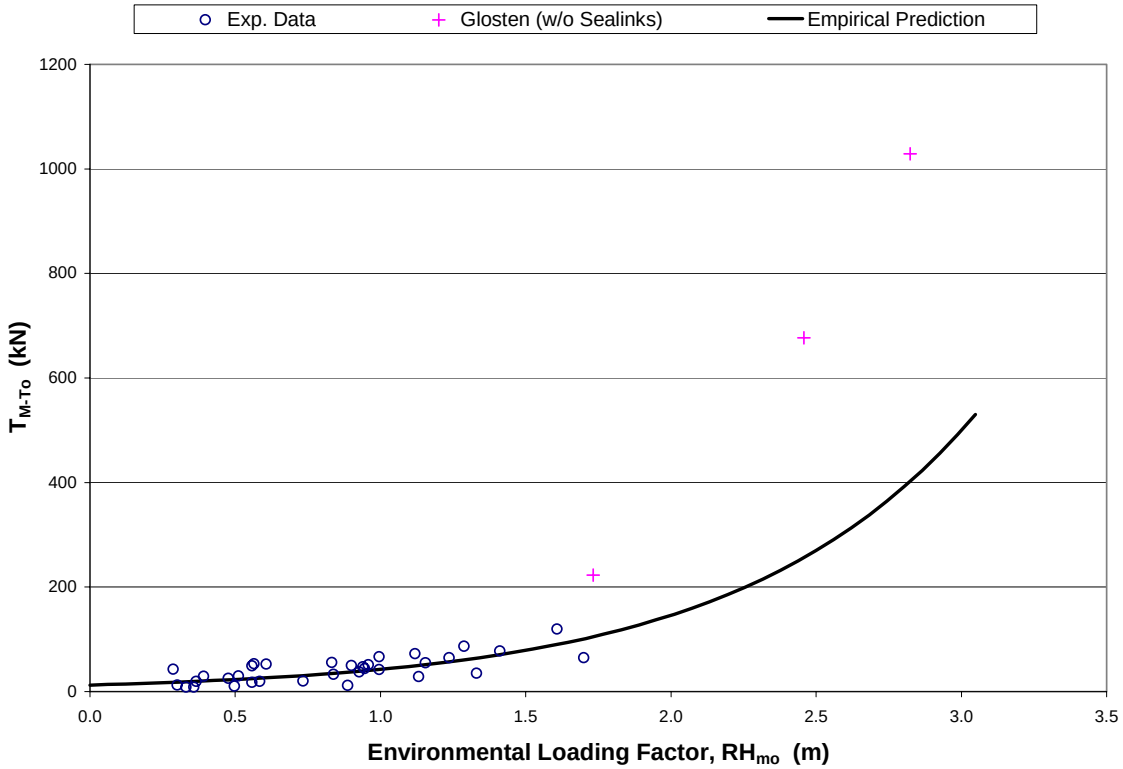

Figure A.1 - $T_{M\text{-}To}$ vs. Environmental Loading Factor, Cable B_s

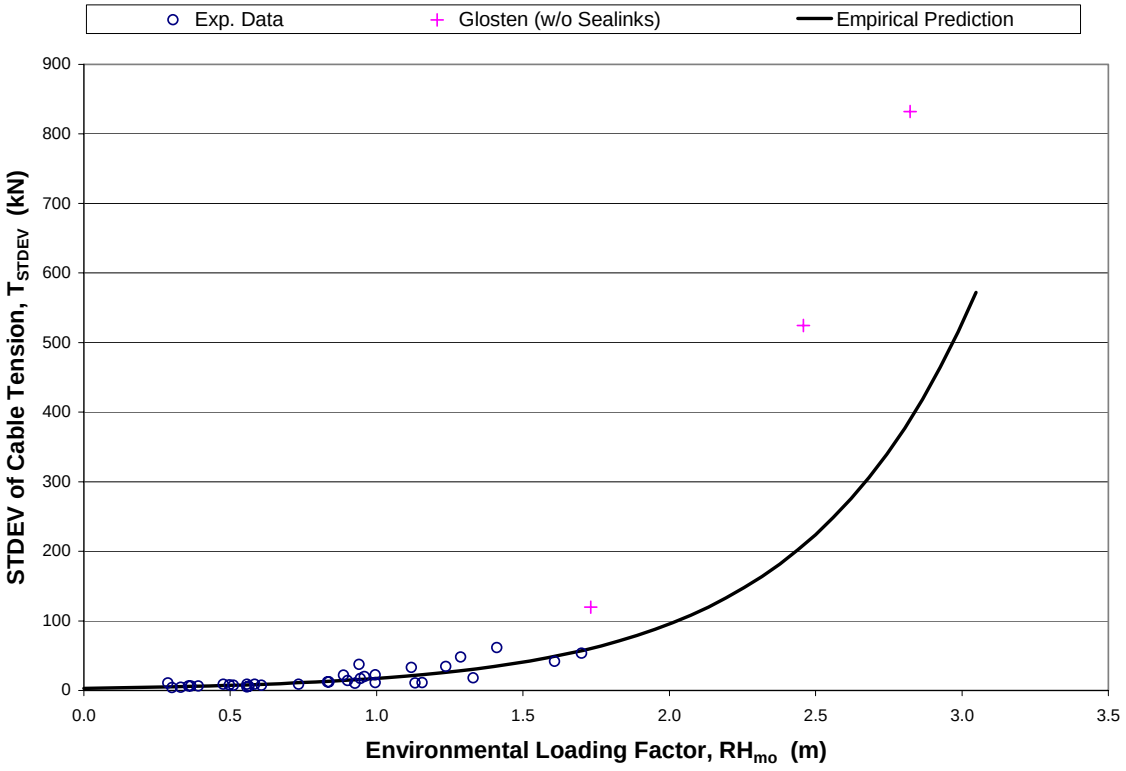

Figure A.2 - T_{STDEV} vs. Environmental Loading Factor, Cable B_s

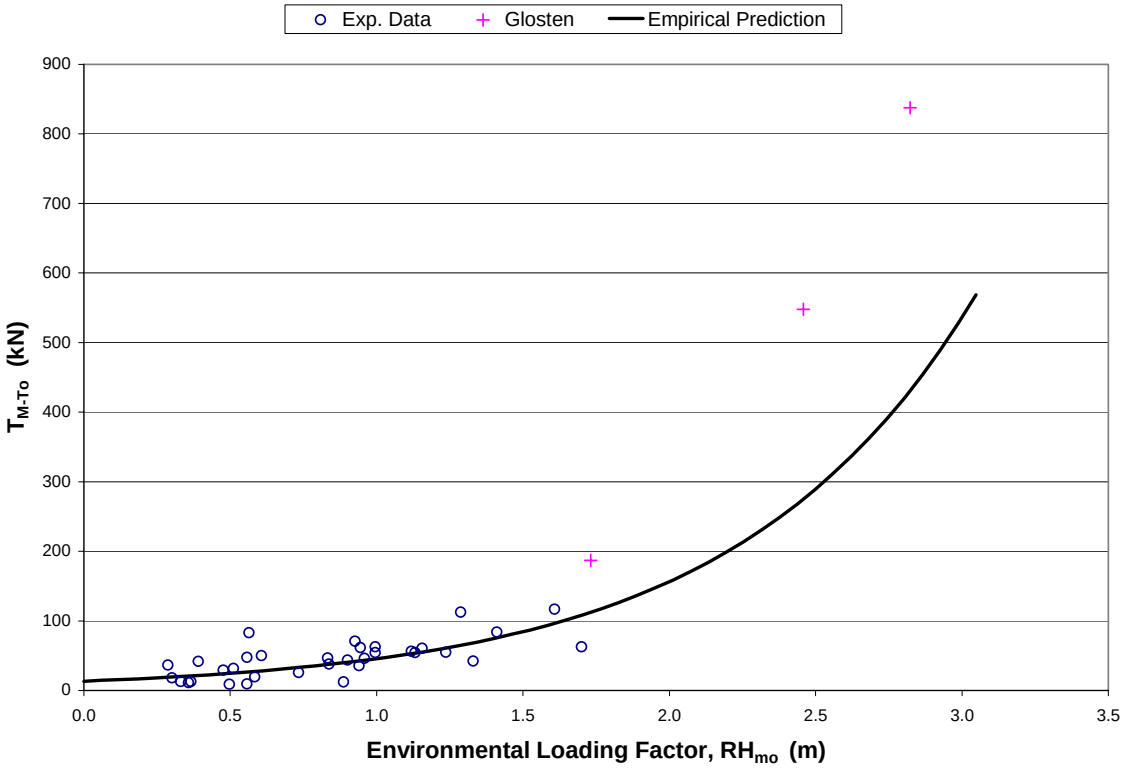

Figure A.3 - $T_{M\text{-}To}$ vs. Environmental Loading Factor, Cable C_s

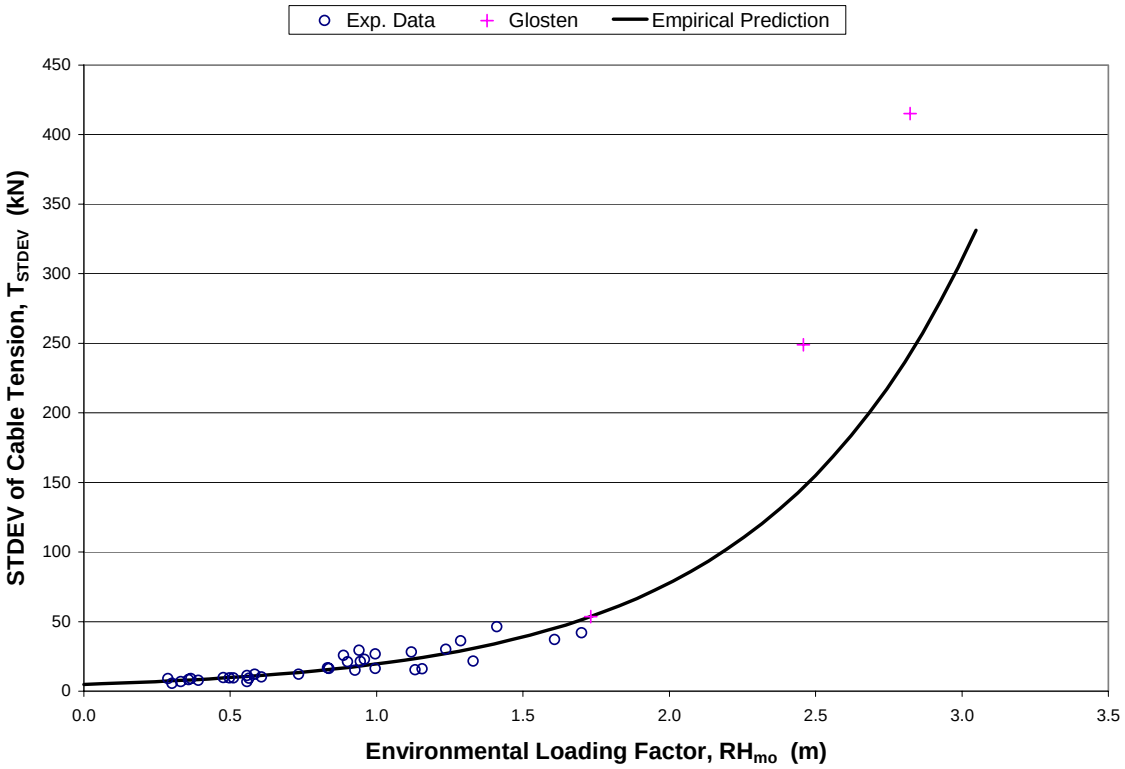

Figure A.4 - T_{STDEV} vs. Environmental Loading Factor, Cable C_s

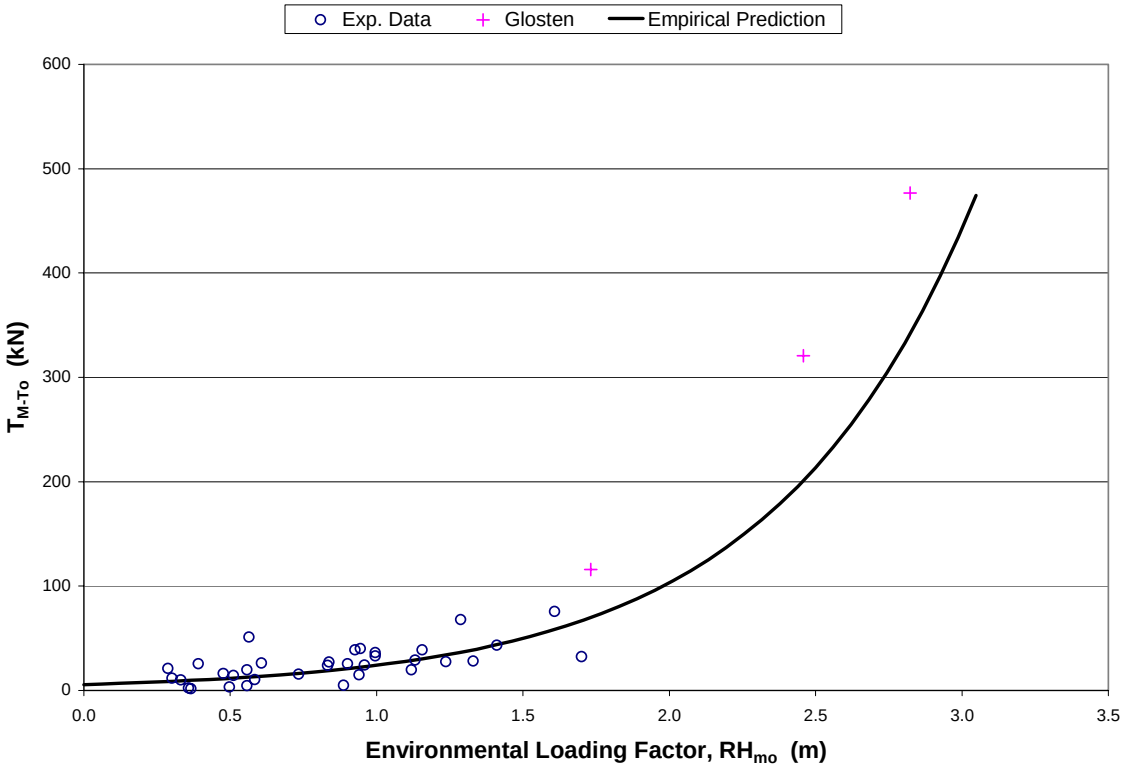

Figure A.5 - $T_{M\text{-}To}$ vs. Environmental Loading Factor, Cable I_s

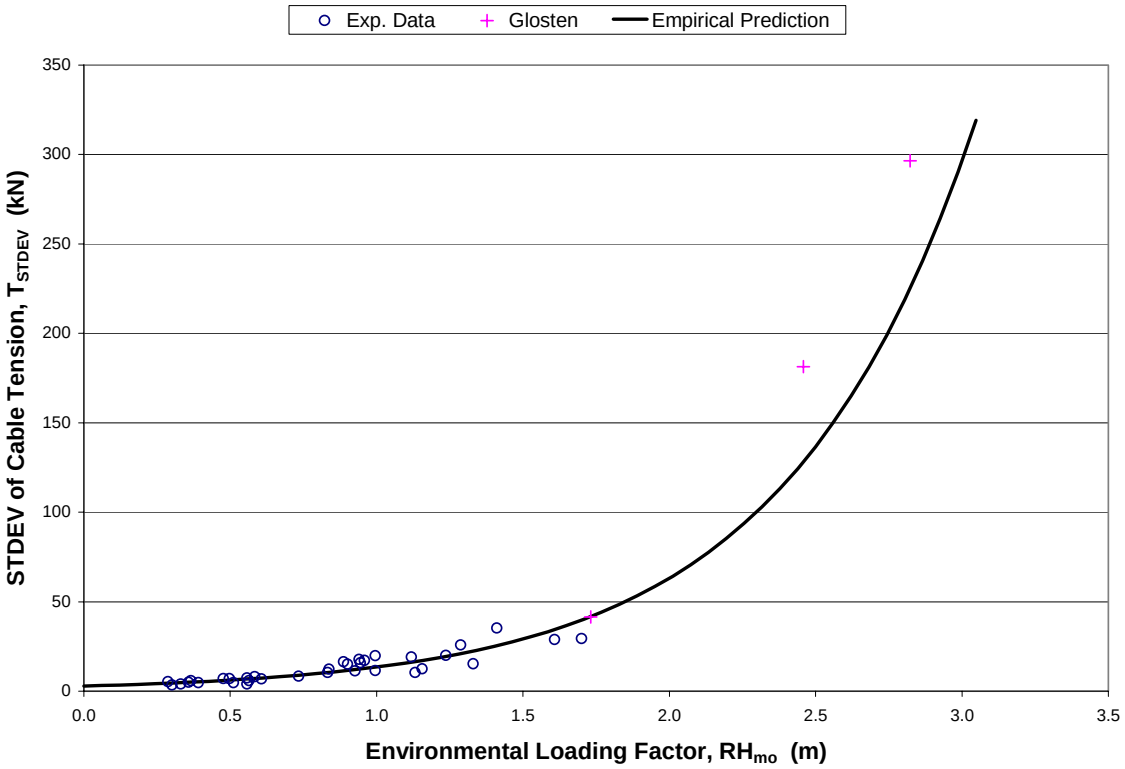

Figure A.6 - T_{STDEV} vs. Environmental Loading Factor, Cable I_s

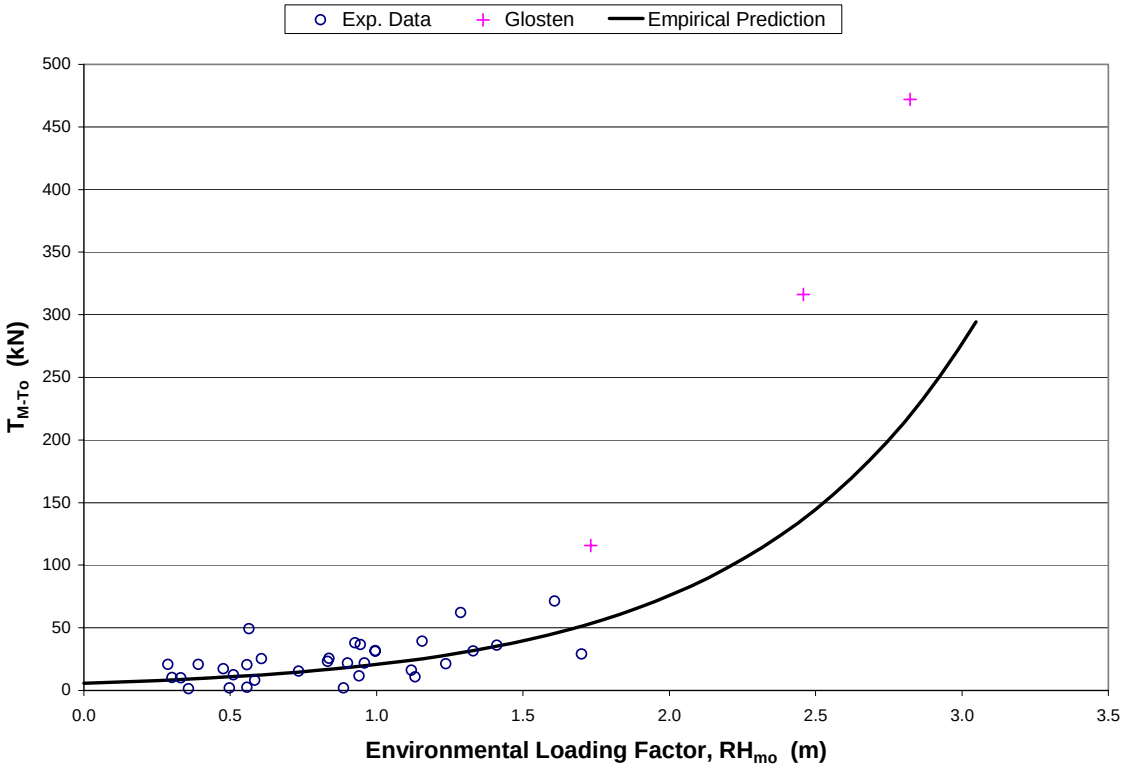

Figure A.7 - $T_{M\text{-}To}$ vs. Environmental Loading Factor, Cable R_s

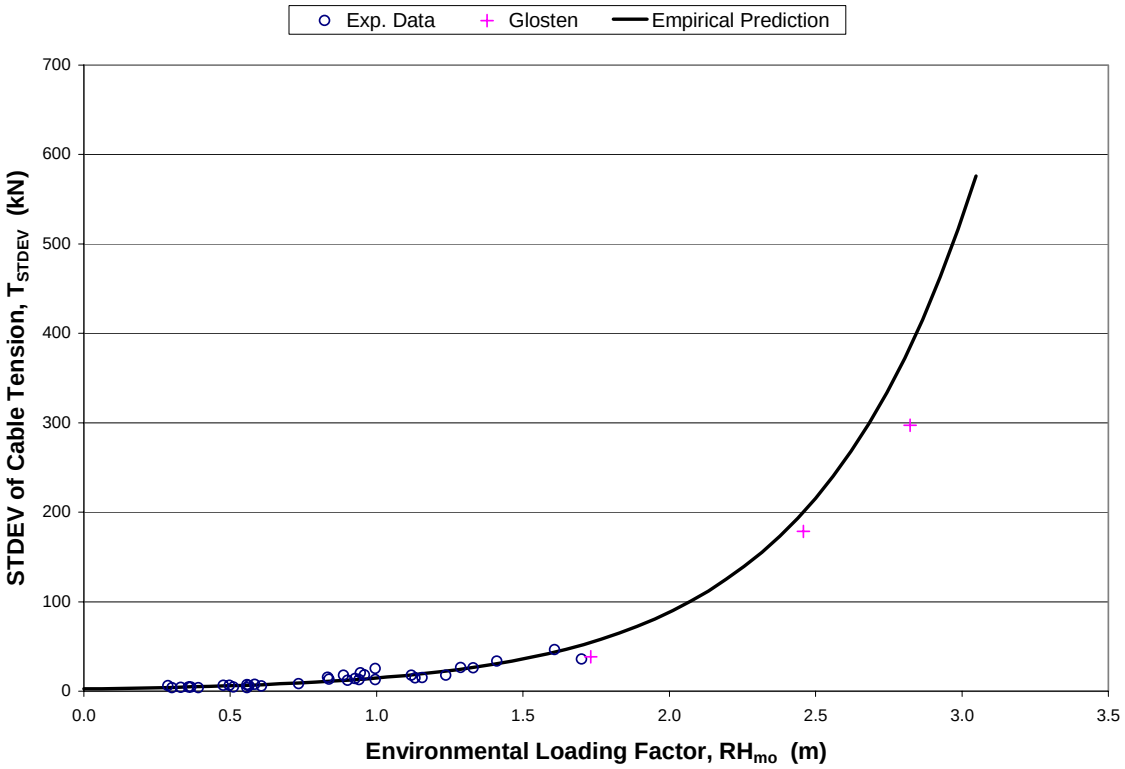

Figure A.8 - T_{STDEV} vs. Environmental Loading Factor, Cable R_s

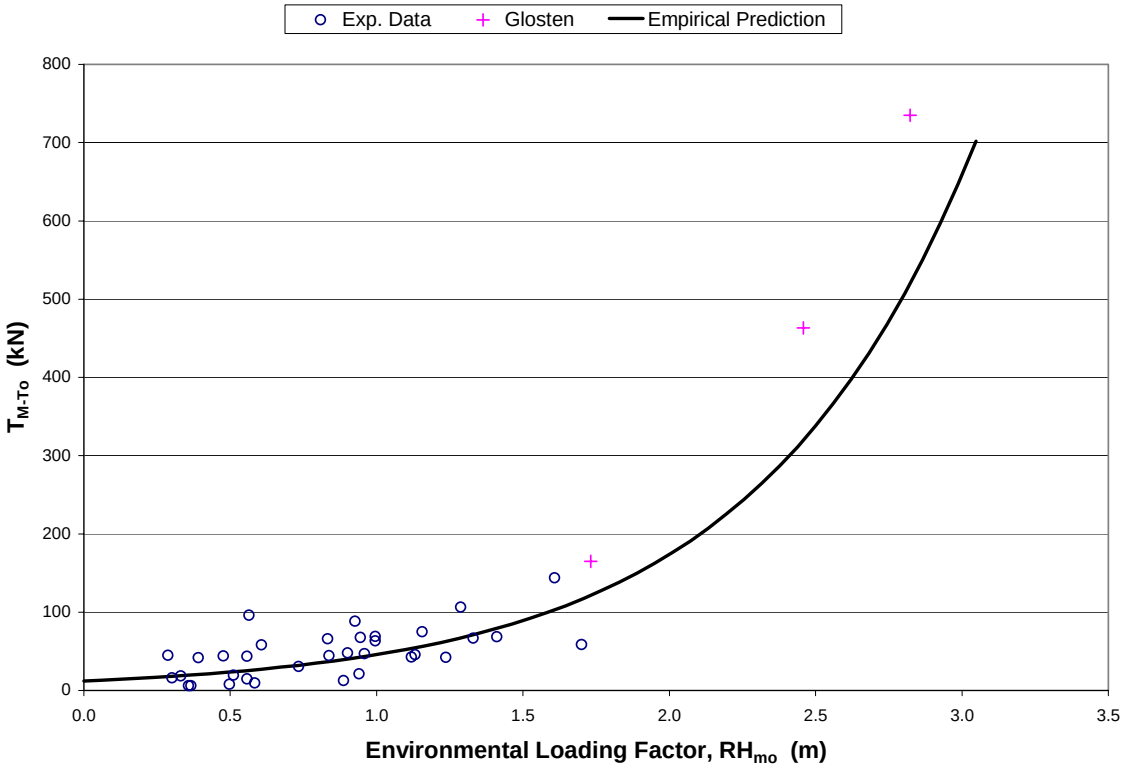

Figure A.9 - $T_{M\text{-}To}$ vs. Environmental Loading Factor, Cable Y_s

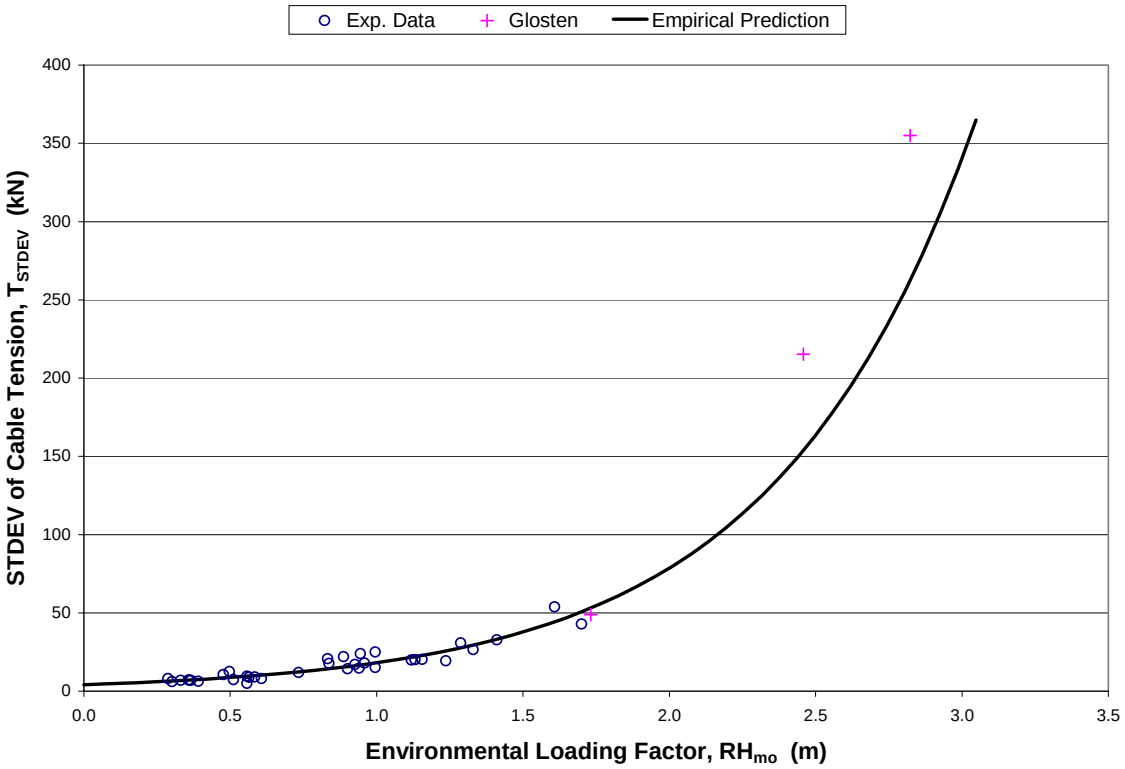

Figure A.10 - T_{STDEV} vs. Environmental Loading Factor, Cable Y_s

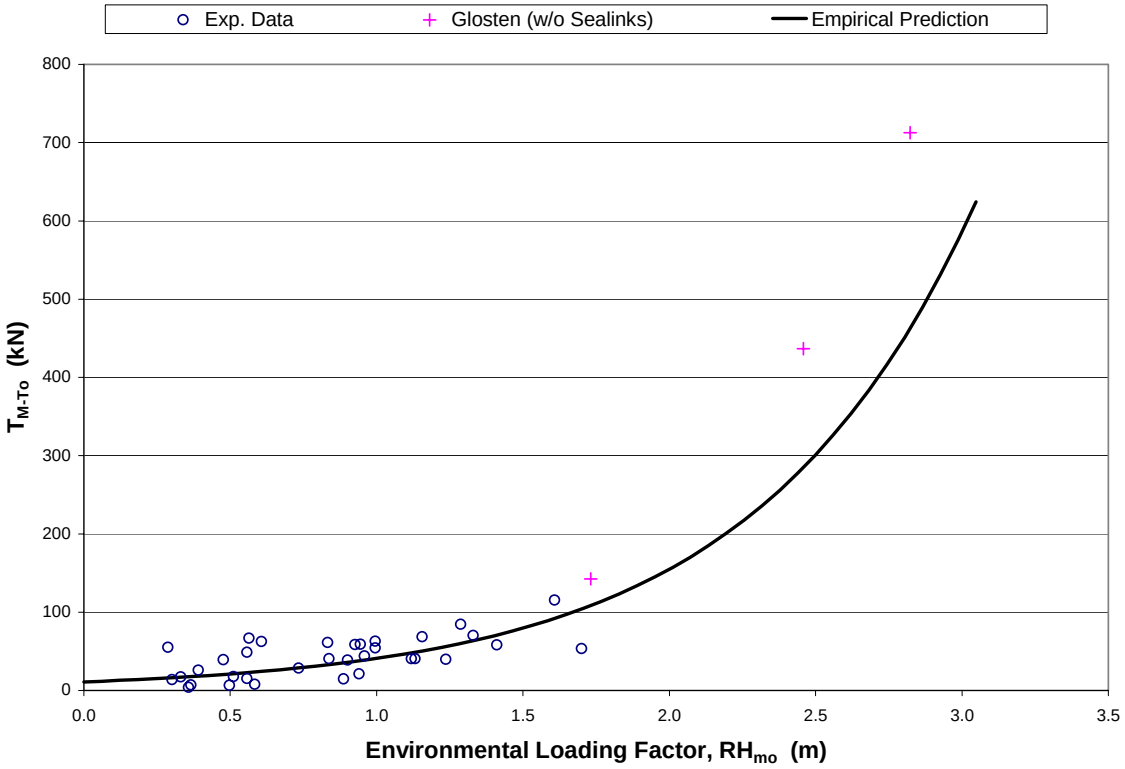

Figure A.11 - $T_{M\text{-}To}$ vs. Environmental Loading Factor, Cable Z_s

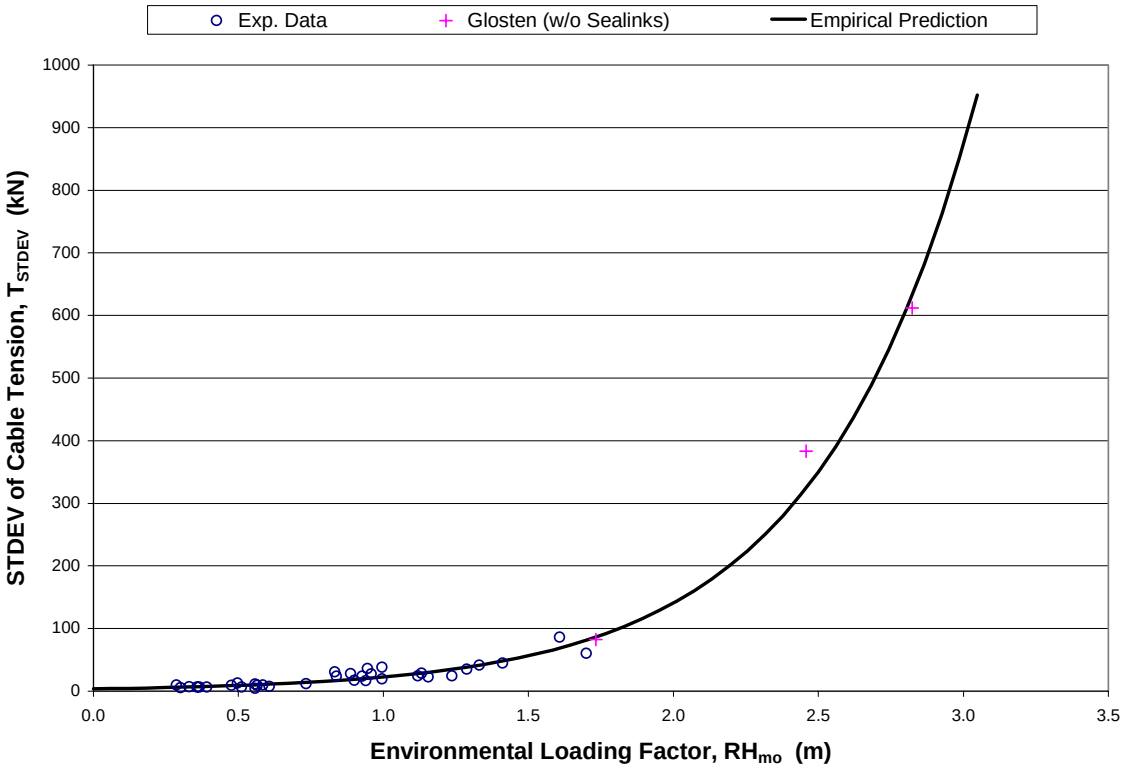

Figure A.12 - T_{STDEV} vs. Environmental Loading Factor, Cable Z_s

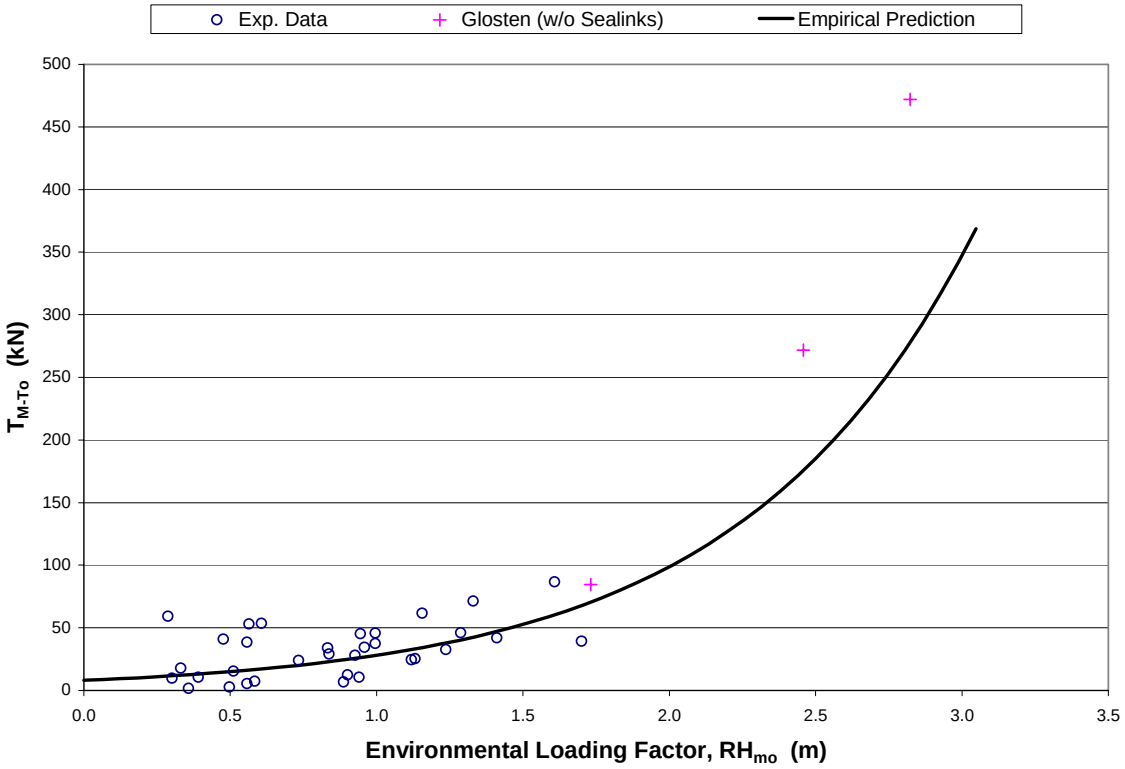

Figure A.13 - $T_{M\text{-}To}$ vs. Environmental Loading Factor, Cable AA_s

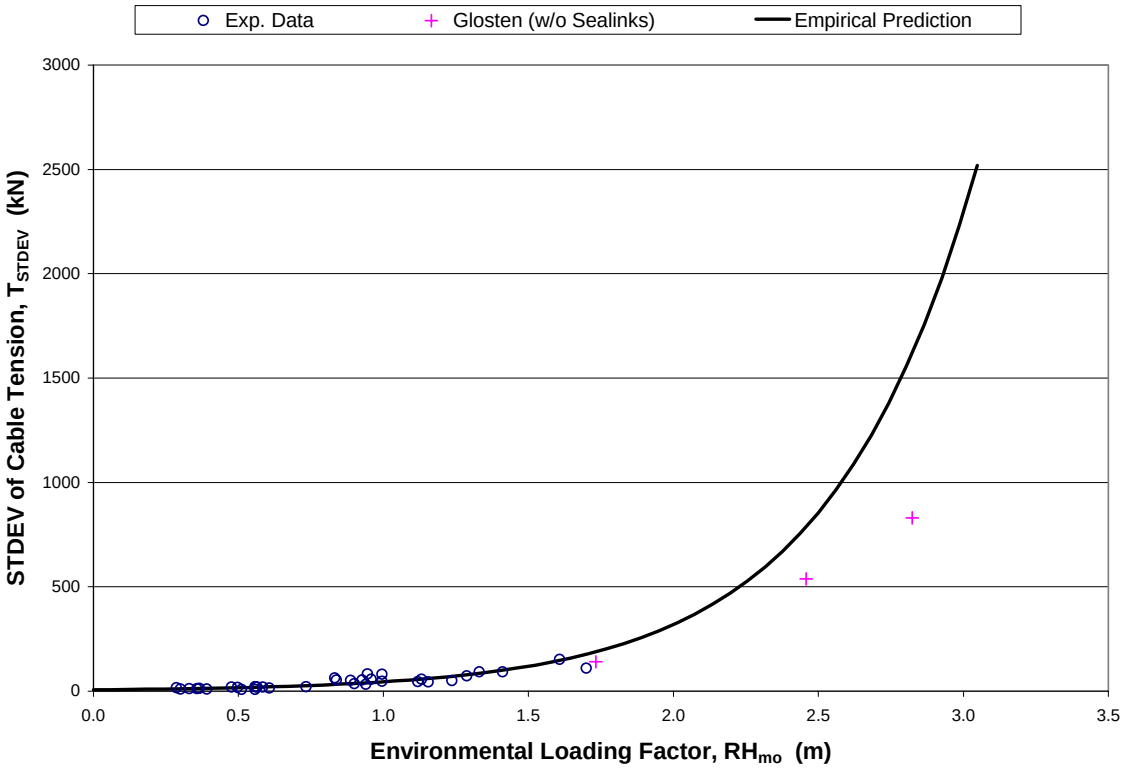

Figure A.14 - T_{STDEV} vs. Environmental Loading Factor, Cable AA_s

APPENDIX B

EPFB MOORING CABLE ANALYSIS PLOTS

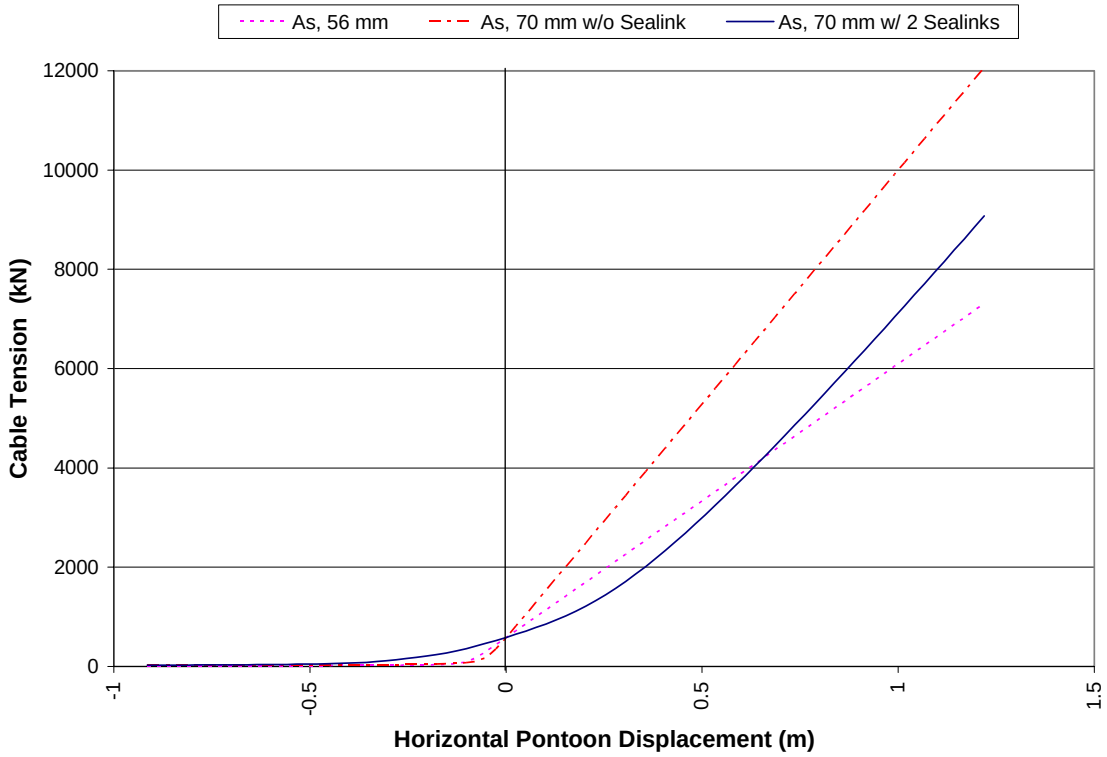

Figure B.1 – Cable Tension vs. Horizontal Pontoon Displacement, Cable A_s

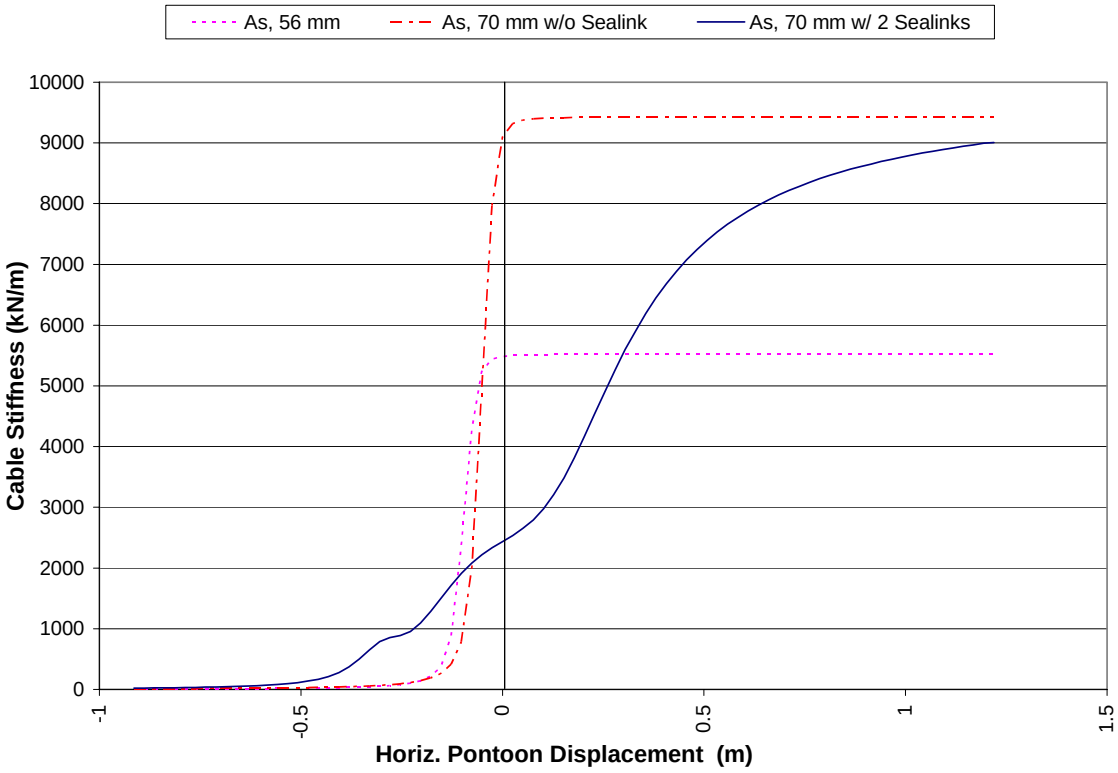

Figure B.2 – Cable Stiffness vs. Horizontal Pontoon Displacement, Cable A_s

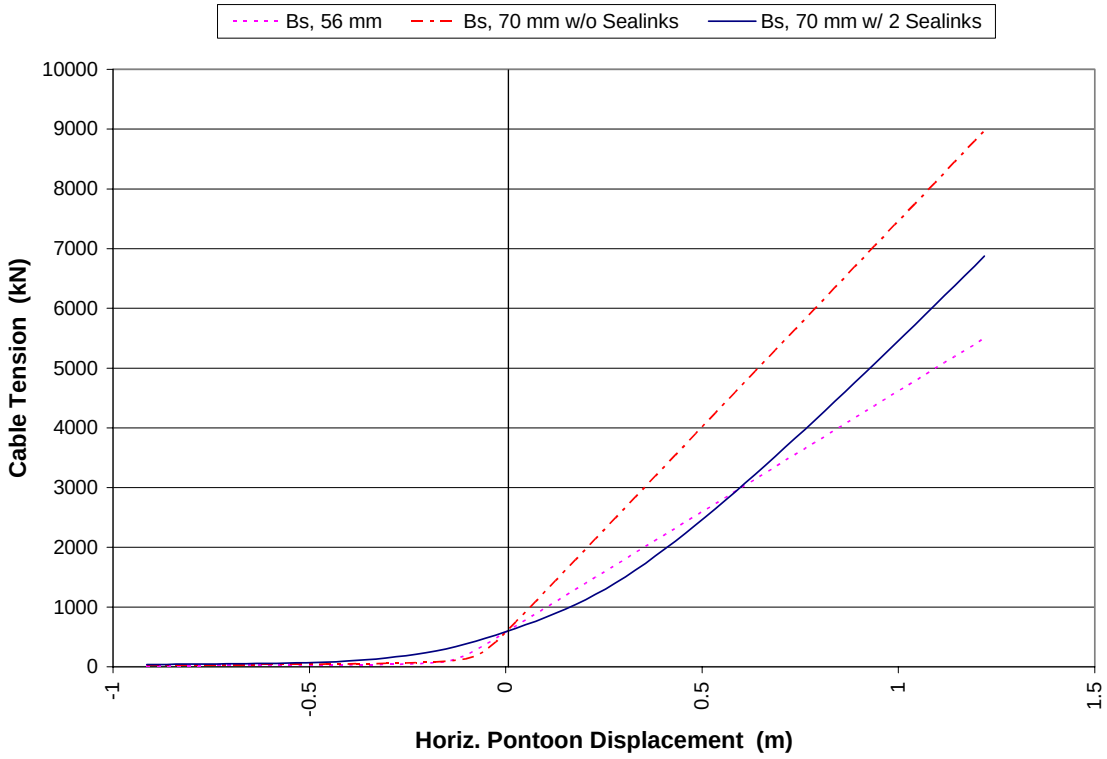

Figure B.3 – Cable Tension vs. Horizontal Pontoon Displacement, Cable B_s

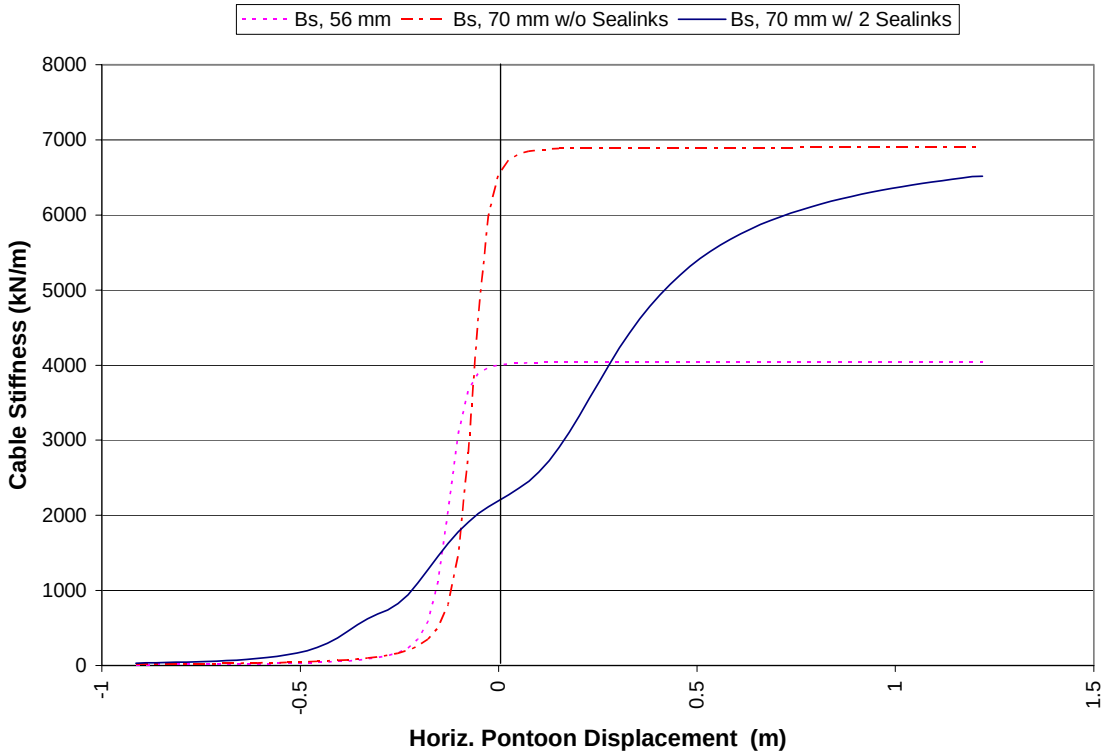

Figure B.4 – Cable Stiffness vs. Horizontal Pontoon Displacement, Cable B_s

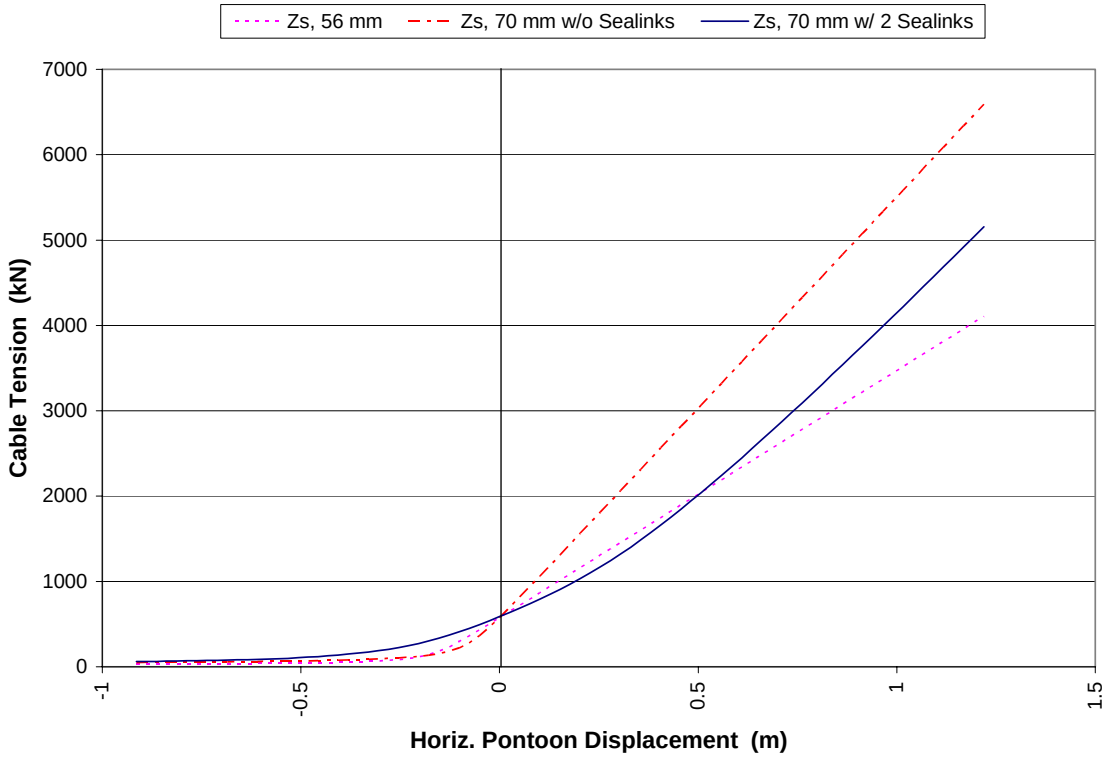

Figure B.5 – Cable Tension vs. Horizontal Pontoon Displacement, Cable Z_s

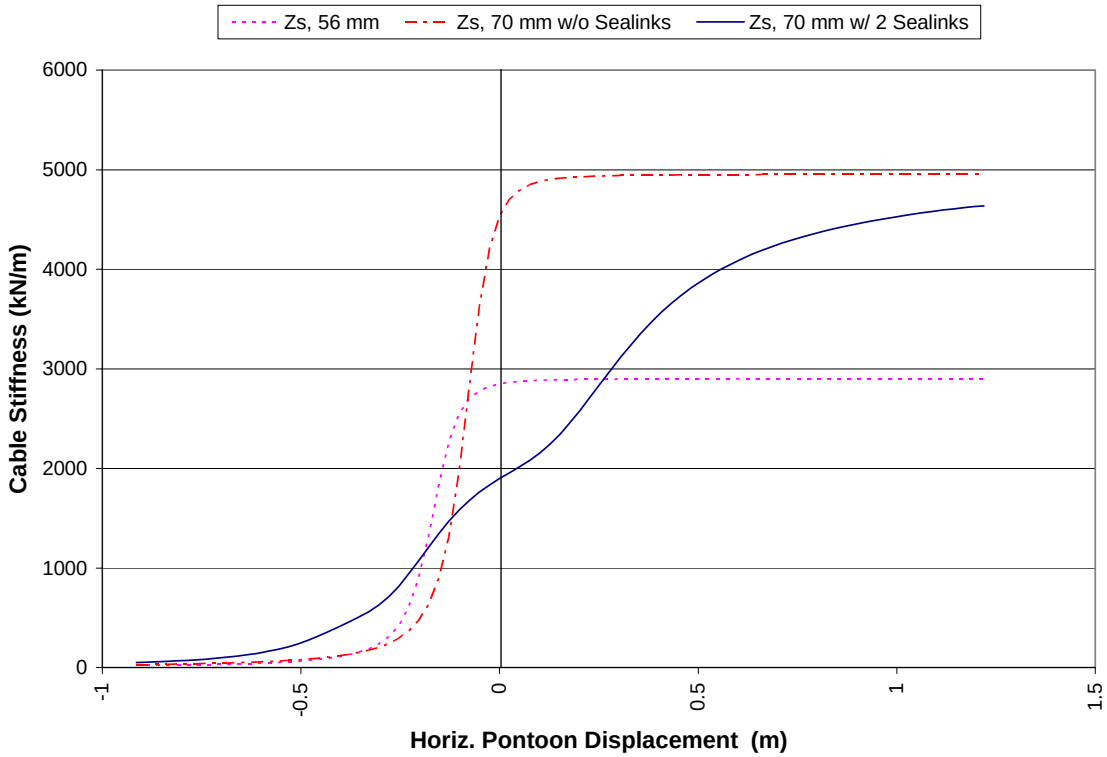

Figure B.6 – Cable Stiffness vs. Horizontal Pontoon Displacement, Cable Z_s

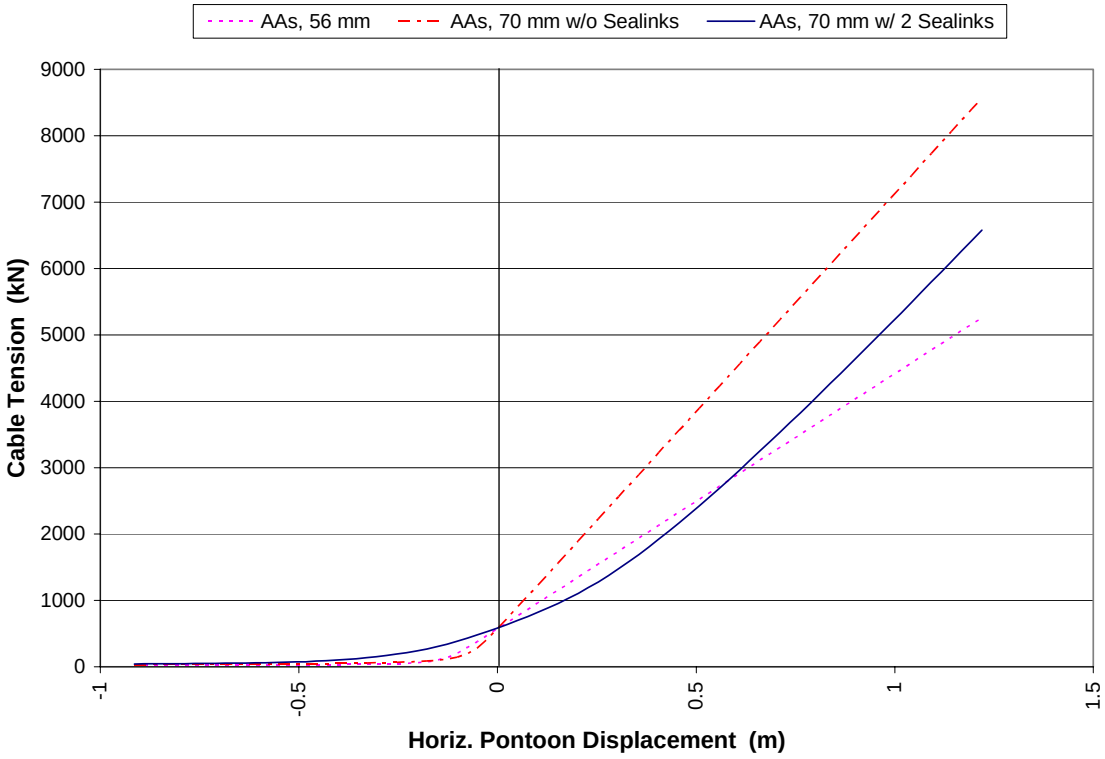

Figure B.7 – Cable Tension vs. Horizontal Pontoon Displacement, Cable AA_s

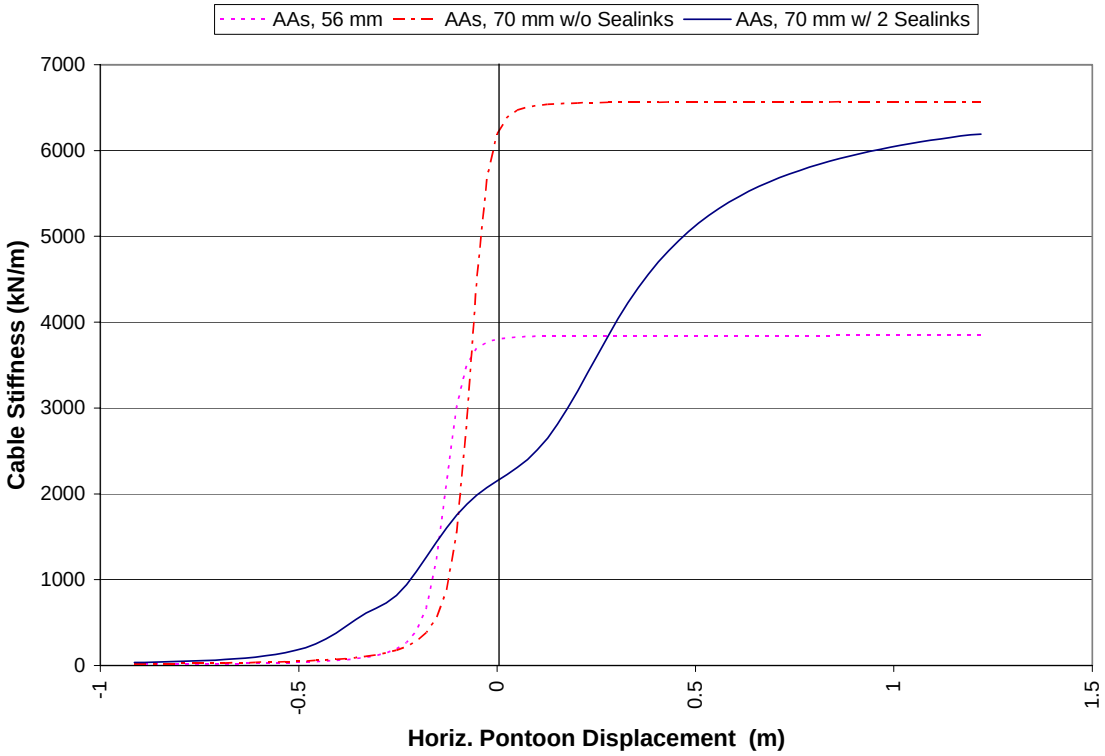

Figure B.8 – Cable Stiffness vs. Horizontal Pontoon Displacement, Cable AA_s